Journal Pre-proofs

Research paper

Formulating elafibranor and obeticholic acid with phospholipids decreases drug-induced association of SPARC to extracellular vesicles from LX-2 human hepatic stellate cells

Cristina Zivko, Finja Witt, Andreas Koeberle, Gregor Fuhrmann, Paola Luciani

PII: S0939-6411(22)00284-3
DOI: https://doi.org/10.1016/j.ejpb.2022.11.025
Reference: EJPB 13912

To appear in: *European Journal of Pharmaceutics and Biopharmaceutics*

Received Date: 26 July 2022
Revised Date: 17 November 2022
Accepted Date: 29 November 2022

Please cite this article as: C. Zivko, F. Witt, A. Koeberle, G. Fuhrmann, P. Luciani, Formulating elafibranor and obeticholic acid with phospholipids decreases drug-induced association of SPARC to extracellular vesicles from LX-2 human hepatic stellate cells, *European Journal of Pharmaceutics and Biopharmaceutics* (2022), doi: https://doi.org/10.1016/j.ejpb.2022.11.025

Formulating elafibranor and obeticholic acid with phospholipids decreases drug-induced association of SPARC to extracellular vesicles from LX-2 human hepatic stellate cells

Cristina Zivko[1,2], Finja Witt[3], Andreas Koeberle[3], Gregor Fuhrmann[4,5], Paola Luciani[1,2]**

[1] Institute of Pharmacy, Friedrich Schiller University of Jena, Jena, Germany
[2] Department of Chemistry, Biochemistry and Pharmaceutical Sciences, University of Bern, Bern, Switzerland
[3] Michael Popp Institute, University of Innsbruck, Innsbruck, Austria
[4] Helmholtz Institute for Pharmaceutical Research Saarland, Department of Pharmacy, Saarland University, Saarbrücken, Germany
[5] Department of Biology, Friedrich-Alexander-University Erlangen, Erlangen, Germany

Prof. Dr. Paola Luciani
University of Bern
Department of Chemistry, Biochemistry and Pharmaceutical Sciences
Freiestrasse 3
3012 Bern, Switzerland
E-mail: paola.luciani@unibe.ch

Prof. Dr. Gregor Fuhrmann
Helmholtz-Institute for Pharmaceutical Research Saarland (HIPS)
University Campus E8 1
66123 Saarbrücken, Germany

Present address:
Friedrich-Alexander-University Erlangen-Nürnberg (FAU)
Pharmaceutical Biology
Department of Biology
Staudstr. 5
91058 Erlangen, Germany
E-mail: gregor.fuhrmann@fau.de

Keywords: extracellular vesicles; SPARC; elafibranor; obeticholic acid; phospholipids

Abstract

Chronic hepatic diseases often compromise liver function and are directly responsible for up to two million yearly deaths world-wide. There are yet no treatment options to solve this global medical need.

Experimental drugs elafibranor (Ela) and obeticholic acid (OA) appeared promising in numerous earlier studies, but they recently struggled to show significant benefits in patients.

Little is known on the drugs' impact on hepatic stellate cells (HSCs), key players in liver fibrogenesis. We recently reported a beneficial effect of polyenylphosphatidylcholines (PPCs)-rich formulations in reverting fibrogenic features of HSCs, including differences in their extracellular vesicles (EVs).

Here, we newly formulated Ela and OA in PPC liposomes and evaluated their performance on the LX-2 (human HSC) cell line through our rigorous methods of EV-analysis, now expanded to include lipidomics. We show that direct treatments with Ela and OA increase EV-associated secreted protein acidic and cysteine rich (SPARC), a matricellular protein overexpressed in fibrogenesis. However, our results suggest that this potentially damaging drugs' action to HSCs could be mitigated when delivering them with lipid-based formulations, most notably with a PPC-rich phospholipid inducing specific changes in the cellular and EV phospholipid composition. Thus, EV analysis substantially deepens evaluations of drug performances and delivery strategies.

1. Introduction

Liver fibrosis is a major global health concern because its evolution into liver cirrhosis is followed by the death of over a million of people every year worldwide [1–3]. The progressive deposition of collagen rich extracellular matrix often develops into cirrhosis, which predisposes patients to hepatocellular carcinoma. At present, at least a third of patients with non-alcoholic steatohepatitis (NASH)-induced cirrhosis die as a result of liver-associated issues within 10 years of their onset [4,5].

The pivotal role of hepatic stellate cells (HSCs, the main collagen-producing cells) in hepatic fibrogenesis makes them interesting from both a therapeutic and a diagnostic perspective. Upon liver insults, these cells undergo transdifferentiation from a quiescent into an activated, fibrotic status to promote wound healing. This becomes medically dangerous when exacerbated by chronic diseases, steadily advancing to a cirrhotic state and culminating in organ failure [6,7].

There is currently no pharmacological treatment specifically approved for liver fibrosis, and the available options for its management are only addressing the underlying cause [8,9]. For example, viral hepatitis is treated with antiviral agents, such as entecavir [10], and excessive hepatic inflammation in autoimmune hepatitis can be successfully managed with steroids [11,12]. When the fibrosis is linked to primary biliary cholangitis (PBC), the use of ursodeoxycholic acid (UDCA) can help delaying the need for liver transplantation, although reports on its benefits are conflicting, and the exploration of novel PBC treatments is underway [13]. Cenicriviroc has been emerging as a candidate drug for patients with NASH, due to its dual antagonism of the chemokine receptors CCR2 and CCR5 (involved in monocyte chemotactic recruitment) [14–16]. Most recently, its application for NASH is being tested along with tropifexor, a highly potent, non-bile acid, farnesoid X receptor (FXR) agonist (regulator of bile acid signaling) [15,17]. Other drugs under investigation include elafibranor (Ela) and obeticholic acid (OA) [18–26]. Numerous studies optimistically explored the potential of both drugs alone and in combination in relieving hepatic fibrogenesis [27,28]. Ela is a peroxisome proliferator-activated receptor PPAR-α and PPAR-δ dual agonist. PPARs are fatty-acid activated transcription factors belonging to the nuclear hormone receptor superfamily, playing a pivotal role in regulating metabolic and energy homeostasis, immune-inflammation, and differentiation [25,29]. PPAR agonists, typically having an amphiphilic structure with a polar head linked to a hydrophobic tail [30], are a class of drugs used for the treatment of metabolic syndrome symptoms (i.e., lowering triglycerides and blood sugar) [31]. Ela has shown high potency in PPAR-α/δ agonism, enhancing fatty acid transport and oxidation, with half maximal effective concentrations (EC_{50}) of 45 nM and 175 nM, respectively [25]. OA, on the other hand, is a semi-synthetic analogue of bile acid, a potent agonist (EC_{50} = 99 nM) of the FXR, a nuclear hormone receptor of key importance in the regulation of bile acid homeostasis and hepatic metabolism [32], and the first such drug used in human clinical studies [33,34]. It has been shown that, besides its beneficial action on hepatocytes, OA contributed to the reduction of

liver fibrosis hallmarks such as α-smooth muscle actin (αSMA) and collagen (col1a1) in rodent models of fibrosis and cirrhosis [35,36]. However, both Ela and OA have struggled in phase 3 clinical trials. Genfit has accordingly decided to refocus Ela approval for PBC alone for now, while revisiting their previous experimental findings [37]. For OA, Intercept Pharmaceuticals was recently denied accelerated approval for the treatment of NASH-related hepatic fibrosis by the Food and Drug Agency [38].

Essential phospholipids (EPLs, purified soy bean extracts) are enriched in polyenylphosphatidylcholines (PPCs), and they have a long history of being used as supportive therapy for fatty liver disease due to their supposed anti-inflammatory effect [39,40]. Even though many questions about their mechanism of action remain open, we have previously reported on the beneficial effect of PPC-rich (>75%) lipid S80 in particular in deactivating perpetuated HSCs [41–43].

The diagnosis of liver fibrosis is equally challenging because the progression of the disease is mostly asymptomatic in its initial stages [42,43]. The current diagnostic gold standard is histopathological assessment upon tissue biopsy, a highly invasive and painful approach [44,45]. Extracellular vesicles (EV) is a collective term referring to a diverse group of small membrane vesicles virtually released by all cell types [46,47]. Given EVs' role in intercellular communication, they have sparked considerable scientific interest into their diagnostic potential [48–50]. For some pathological dispositions, EVs can be applied as liquid biopsies as they are enriched in selected biomolecules and they are intrinsically equipped to protect their cargo from degradation. Despite their complexity of characterization, they are still easier to analyze than total blood or serum samples [51–53].

We aimed to thoroughly analyze EVs shed by a human cell line of HSCs, the LX-2 cells, in different phenotypical states, potentially paving the way to non-invasive and less painful methods for the evaluation of liver fibrosis therapy. In recent work, we have documented the successful establishment of rigorous methodological practices for the isolation, purification and

characterization of LX-2 EVs [54]. These included extensive proteomic analyses, which also led to the development of a user-friendly fluorescence nanoparticle tracking analysis (f-NTA) method for the assessment of treatment effect by EV-analytical evaluation. The relative abundance of one biomarker we selected, the secreted protein acidic and cysteine rich (SPARC), associated to EVs was greatly reduced upon treatment with S80, while pro-fibrotic treatment with transforming growth factor β1 (TGF) did the opposite.[54] With the present study we extend our portfolio of EV-analytical methodologies to lipidomics profiling. With this expanded arsenal we aimed to evaluate the response of HSCs to pharmacological treatments. We selected Ela and OA to look into their impact specifically on HSCs and HSC-derived EVs, about which still very little is known [55], thus shedding new light on previous enthusiastic reports about the two drugs. Our results indicate negative effects of direct treatments with Ela and OA on HSCs, as seen through our novel, EV-based screening method. However, this also enabled us to evaluate a possible strengthening of the drugs' otherwise reported antifibrotic action, by means of a coformulation with the phospholipid S80. To better investigate *in vitro* their effect on HSCs, we decided here to load the drugs in S80 liposomes. We could thus effectively use EV-analysis to provide novel perspectives into the performance of experimental therapeutic agents, and also to assess improvements provided by the co-treatment with PPCs.

Overall, our findings suggest that PPC-rich bioactive phospholipids such as S80 could be considered as excipients in solid dosage forms to improve the therapeutic efficacy of investigational antifibrotic drugs such as OA or Ela in the long-term treatment of chronic liver diseases.

2. Materials and methods

Formulation and characterization of drug-loaded PPC-based liposomes. Liposomal formulations were prepared by the thin film hydration method as previously described [41]. Briefly, suitable aliquots of S80 or DOPC were dissolved with $CHCl_3$, the organic solvent was removed with a nitrogen stream, and left under vacuum overnight. The resulting lipid film was hydrated with 10 mM HEPES buffer pH 7.4 and, for drug-loaded liposomes, the appropriate amount of Ela or OA (from 100 mM stock solutions in MeOH) was added. The resulting multilamellar vesicles subjected to six freeze-thaw cycles. The liposomes were then extruded 10 times through a 200 nm polycarbonate membrane at room temperature with a Lipex® extruder (Evonik Health Care). Lipids (final concentration 50 mM) and drugs (up to 150 µM) concentrations were quantified chromatographically, as previously reported [41,56]. Briefly, samples were diluted with MeoH 1:49 (v/v) to destroy lipid vesicles prior to injection in an Ultimate 3000 HPLC system (Thermo Fisher Scientific), equipped with a charged aerosol detector (CAD, Corona Veo RS, Thermo Fisher Scientific). The column was a MN Nucleosil (C18, 3.0 x 125 mm, 5 µm, Macherey Nagel), used at 30 °C. Samples were run with a flow rate of 0.5 mL/min. For the mobile phase, solvent A was ACN:H2O 90:10 (v/v) with 0.05% TFA (v/v), and solvent B was MeOH with 0.05% TFA (v/v). The method was isocratic (Solvent A:Solvent B, 60:40) for 25 min, followed by a linear gradient of solvent B over 15 min (from 40 to 100%). The analysis was carried out with Chromeleon 7.2 software (Thermo Fisher Scientific).

The hydrodynamic diameter and the size distribution (polydispersity index, PDI) of the liposomes were measured with a Litesizer 500 (Anton Paar), and their stability at 4 °C was tested for up to 28 days.

Cell culture and treatments. LX-2 cells (passage number 7-16) were grown as previously described in high glucose (4’500 mg/L) DMEM (Carl Roth) supplemented with 200 mM L-Glutamine (Sigma), 10’000 units/L of penicillin and streptomycin (Gibco), and 2% (v/v) of

sterile filtered (0.2 μm, cellulose acetate membrane) fetal bovine serum (FBS, Merck Millipore). For experiments, 0.8-1 x 10^6 LX-2 were seeded in T175 cell culture flasks and cultured for 120 h, or 1 x 10^5 cells/well were seeded in 12-well microtiter plates, or 1 x 10^4 cells/well microtiter plates, and cultured for 24 h. Cells were then washed with phosphate buffered saline (PBS, pH 7.4) and treated for 24 h with different solutions prepared in serum free cell culture media (DMEM): ROL/PA (10/300 μM), TGF (10 ng/mL), HEPES pH 7.2 (10% v/v), Ela or OA (0.025-75 μM in DMEM), liposomal formulations of S80 or DOPC (always freshly prepared, 5 mM lipid concentration in DMEM with 10% v/v HEPES pH 7.2) with or without 150 nM of either Ela or OA.

Cell metabolic activity assay. The CCK-8 assay was used following the manufacturer's instruction, with cells seeded in 96-wells plates (10^4 cells/well). Briefly, cells were washed twice with PBS after treatment with different amounts of Ela and OA (0.025-75 μM); controls for the highest DMSO concentrations (0.088% and 0.075% v/v in DMEM, for Ela and OA respectively) were performed as well. A volume of 90 μL DMEM and a volume of 10 μL of CCK-8 were added to each well. LX-2 were incubated for further 2 h at 37 °C, 5% CO_2. Afterwards, the absorbance was measured at 450 nm using an Infinite 200®Pro (F Plex) Tecan plate reader at 37 °C.

Analysis of lipid droplet content upon treatment with drug-loaded PPC-based formulations. ORO/DAPI staining was performed in 12-wells plates as described [54], but with an initial seeding density of 1 x 10^5 cells/well (as previously reported) [41]. Two concentrations of Ela and OA could be tested (either alone or with S80 and DOPC). The first was a final concentration of 150 nM on the cells (around both drugs' EC_{50} values) and the second one was a final concentration of 50 μM (the lowest quantifiable by HPLC). Since the liposomes were not prepared under sterile conditions, all treatment solutions in DMEM were sterile filtered (CA, 200 nm).

EV isolation. EVs were purified as previosly detailed [54]. Briefly, LX-2 cells were treated with different solutions in serum free conditions for 24 h, after which they were washed once with PBS and supplied with fresh, serum free, cell culture medium regardless of previous treatment. After 24 h more, the EV-containing medium was collected to undergo two rounds of differential centrifugation. The first was 300 x g for 3 min at 4 °C, discarding the pellet; the second was 9'000 x g for 30 min at 4 °C (again, discarding the pellet). This was followed by an ultracentrifugation step (120'000 x g for 2.5 h at 4 °C), after which the EV-containing pellet was re-suspended in 0.5 mL of PBS and purified by size exclusion chromatography (SEC) for further analysis.

Sample preparation for lipidomic analysis. LX-2 cells were treated with DMEM, ROL/PA (10/300 μM in DMEM), TGF (10 ng/mL in DMEM), HEPES buffer pH 7.2 (10% v/v in DMEM), Ela (150 nM in DMEM), OA (150 nM in DMEM), S80 (5 mM in DMEM with 10% v/v HEPES pH 7.2), S80+Ela (5 mM+150 nM respectively, in DMEM with 10% v/v HEPES pH 7.2), S80+OA (5 mM+150 nM respectively, in DMEM with 10% v/v HEPES pH 7.2), DOPC (5 mM in DMEM with 10% v/v HEPES pH 7.2), DOPC+Ela (5 mM+150 nM respectively in DMEM with 10% v/v HEPES pH 7.2) and DOPC+OA (5 mM+150 nM respectively in DMEM with 10% v/v HEPES pH 7.2) at 37°C and 5% CO_2. After 24 h, cells were washed with PBS pH 7.4 and supplemented with fresh serum free DMEM regardless of previous treatment. After 24 h, cells and EVs were harvested and phospholipids and FFA were extracted on ice as previously described [54]. In brief, the internal standards PC(14:0/14:0) (DMPC), PE(14:0/14:0) (DMPE), PG(14:0/14:0) (DMPG) and (15,15,16,16,17,17,18,18,18-d9)oleic acid (d9-18:1) (0.2 nmol, each; Avanti Polar Lipids) were given to samples in 1 mL aqueous PBS pH 7.4. Methanol (2.43 mL), $CHCl_3$ (2× 1.25 mL), saline (1.25 mL) were successively added and each step was accompanied by vigorous mixing. After centrifugation (6500 × g, 5 min, 4 °C), the lower phase was recovered, concentrated under nitrogen, and stored at -20 °C. Lipids were dissovled in methanol and subjected to UPLC-MS/MS analysis. For

SEC-purified samples, 1 mL of column eluent was collected prior to EV-pellet loading and extracted and analyzed as quality control.

Targeted lipidomics by UPLC-MS/MS. Chromatographic separation of phospholipids and fatty acids was achieved using an Acquity UPLC BEH C8 column (1.7 µm, 2.1×100 mm, Waters, Milford, MA) and an ExionLC™ AD UHPLC system (Sciex). The mobile phase was composed of A (acetonitrile/water, 95/5, 2 mM ammonium acetate) and B (water/acetonitrile, 90/10, 2 mM ammonium acetate) and delivered at a flow rate of 0.75 ml/min. Starting from A/B = 75/25, the gradient raised to 85% of mobile phase A within 5 min and was followed by isocratic elution at 100% mobile phase A for 2 min. The column temperature was adjusted to 45 °C. LC-separated lipids were ionized in an electrospray ionization (ESI) source and detected by multiple reaction monitoring (MRM) (glycerophospholipids) or multiple ion monitoring (free fatty acids) in the negative ion mode using a QTRAP 6500^{+} Mass Spectrometer (Sciex) [57,58]. Both fatty acid anion fragments were determined for the analysis of glycerophospholipids, and the average of both transitions was used for quantitation. The system was operated with following settings: curtain gas at 40 psi, collision gas set to medium and an ion spray voltage of 4500 V in the negative mode. The temperature of the heated capillary ranged from 350 °C (PC) to 650 °C (PE), the sheath gas pressure was set to 55 (PC, PE, PG, PI) or 60 psi (FFA) and the auxiliary gas adjusted to 75 – 80 psi.

The total amount of lipid classes (PC, PE, PG, PI, FFA) was calculated as sum of the individual signal intensities of the lipid species analyzed for the indicated lipid class. Lipid species were normalized to the internal standard d9-18:1, and class-specific differences were corrected by external calibration using lipid class specific standards [i.e., PC(14:0/14:0), PE(14:0/14:0), and PG(14:0/14:0)]. The proportions of individual lipids [e.g., PC(18:0/18:2)] were instead calculated as percentage of the summarized total signal intensity of a given lipid class (e.g., PC).

Detection of EV-associated SPARC by fluorescence nanoparticle tracking analysis. EVs were incubated with AlexaFluor®488 conjugated anti-human SPARC antibody (AF488-SPARC, mouse IgG1 Clone #122511, Biotechne) as reported before [54]. Briefly, EV-pellets were incubated with 8 ng/mL of AF488-SPARC for 5 h at 24 °C, and they were subsequently purified by SEC. The different treatments the cells were subjected to prior to EV-harvest were the following: DMEM, ROL/PA (10/300 μM), TGF (10 ng/mL), HEPES buffer (10% v/v in DMEM), Ela (150 nM in DMEM), OA (150 nM in DMEM), S80 (5 mM in DMEM with 10% v/v), S80+Ela (5 mM+150 nM), S80+OA (5 mM+150 nM) DOPC (5 mM), DOPC+Ela (5 mM+150 nM) and DOPC+OA (5 mM+150 nM).

Statistical analysis. All experiments were performed in at least three independent replicates, and samples were always freshly prepared.

One-way ANOVA analysis of variance was used to compare means of independent experiments. Significant differences in lipid droplets quantification following the various treatments were compared by Tukey's multiple comparisons test (**** $p \leq 0.0001$, *** $p \leq 0.001$, ** $p \leq 0.01$, *$p \leq 0.05$). Data are presented as mean ± S.D.

3. Results and Discussion

3.1 Formulation of drug-loaded liposomes and cell toxicity assay

The formulation of drug-loaded liposomes with Ela and OA underwent a stepwise assessment of its feasibility. OA and Ela were shown to be stable to freeze-thaw (FT) cycles, required for the production of unilamellar liposomes (**Figure S1,2**), and quantified by HPLC coupled to a charged aerosol detector (CAD, retention time t_R Ela: 1.036 min; t_R OA: 1.308 min) (**Figure S3**). Choosing 50 µM as our lowest, quantifiable, final drug concentration, we evaluated drug encapsulation efficiency (EE%) to be >83% (**Figure 1**). Upon extrusion, the average size of the produced lipid vesicles was around 150 nm and monodisperse, as evidenced by the measured PDI values.

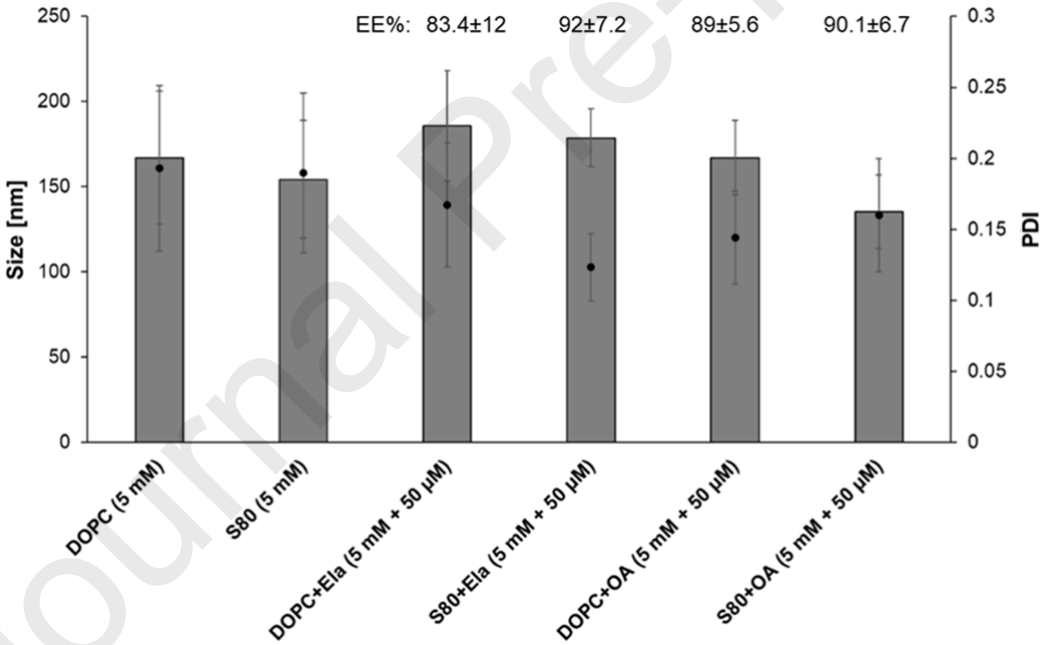

Figure 1. Average size, PDI and EE% for the different liposomal formulations immediately after preparation. Mean ± SD, n = 3-6.

Cell metabolic activity was determined by measuring mitochondrial dehydrogenase activity, and the results showed no visible effect in the tested concentration range (**Figure 2**). Thus, for further experiments on cells, we chose to test a final concentration of drugs of 150 nM (around both drugs' EC_{50} values [25]).

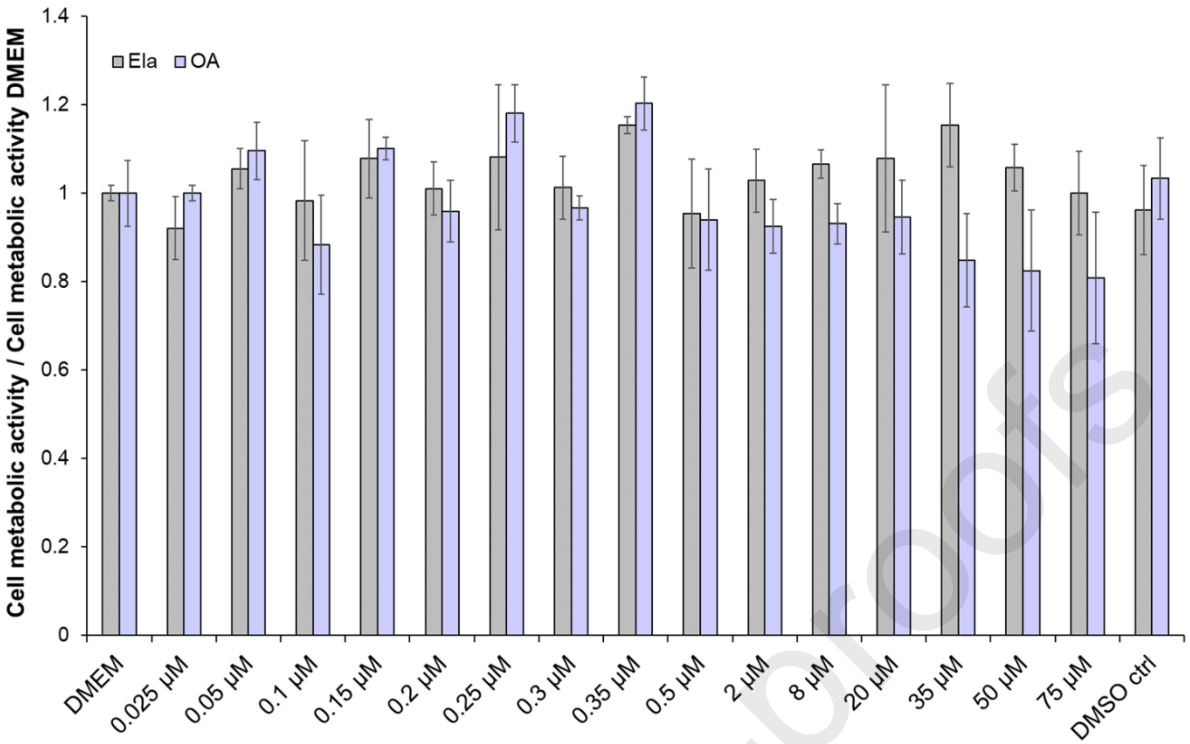

Figure 2. Cell metabolic activity normalized to DMEM, measured with CCK-8 assay on 10'000 cells/well, after 24 h treatment as function of Ela and OA concentration (from 0.025 µM to 75 µM). Controls for the highest DMSO concentrations (0.088% and 0.075% v/v in DMEM, for Ela and OA respectively) were performed as well (DMSO ctrl). Mean ± SD, n = 3-6.

3.2 Analysis of lipid droplet content

In a previous study we screened the concentrations of S80 and the hepatoprotectant silymarin on LX-2 cells by monitoring the progressive increase of cytoplasmic lipid droplets within them [41]. This approach could work for Ela and OA if they have a synergistic effect directly related to the eventual accumulation of lipids in HSCs' cytoplasm, as proven for silymarin. However, though PPARs have been proposed to modulate HSC activation, this hypothesis still needs to find confirm in steatohepatitis-mediated fibrosis.[59] Similarly, the putative effect of farnesoid X receptor agonist on HSC activation, either direct or indirect, has been justified only by a reduced expression of α-1 type 1 collagen in farnesoid X receptor deficient mice [60].

In our previous work [41], we also reported that the combination of retinol and palmitic acid (ROL/PA) stimulates the formation of lipid droplets by an upregulation of the adipose differentiation-related protein, indicating LX-2 cell quiescence. We also showed that the PPC-

containing S80 liposomes, in presence and absence of silymarin, are able to deactivate LX-2 to a non-fibrogenic status.

The control treatments validated in the current project are shown (**Figure 3**): native LX-2 (treated either with DMEM or HEPES 10%); quiescent-like HSCs (LX-2 treated with ROL/PA); perpetuated HSCs (LX-2 treated with TGF); liposome-treated LX-2 (S80 liposomes: positive control, antifibrogenic; DOPC: negative control, expected to be as DMEM or HEPES 10%). These images were then quantitatively analyzed and used as a baseline to evaluate the antifibrogenic effect of the candidate hepatoprotectors OA and Ela.

As expected, cells treated with ROL/PA and S80 display significantly more lipid droplets than with any other treatment group, as evidenced by Oil Red O (ORO) staining (**Figure 3**). PPC formulations that were loaded with OA or Ela showed a remarkable increase in the amount of lipid droplets, while none with DOPC. However, we could not detect a synergistic effect between S80 and either drug in terms of lipid droplets formation when using 150 nM.

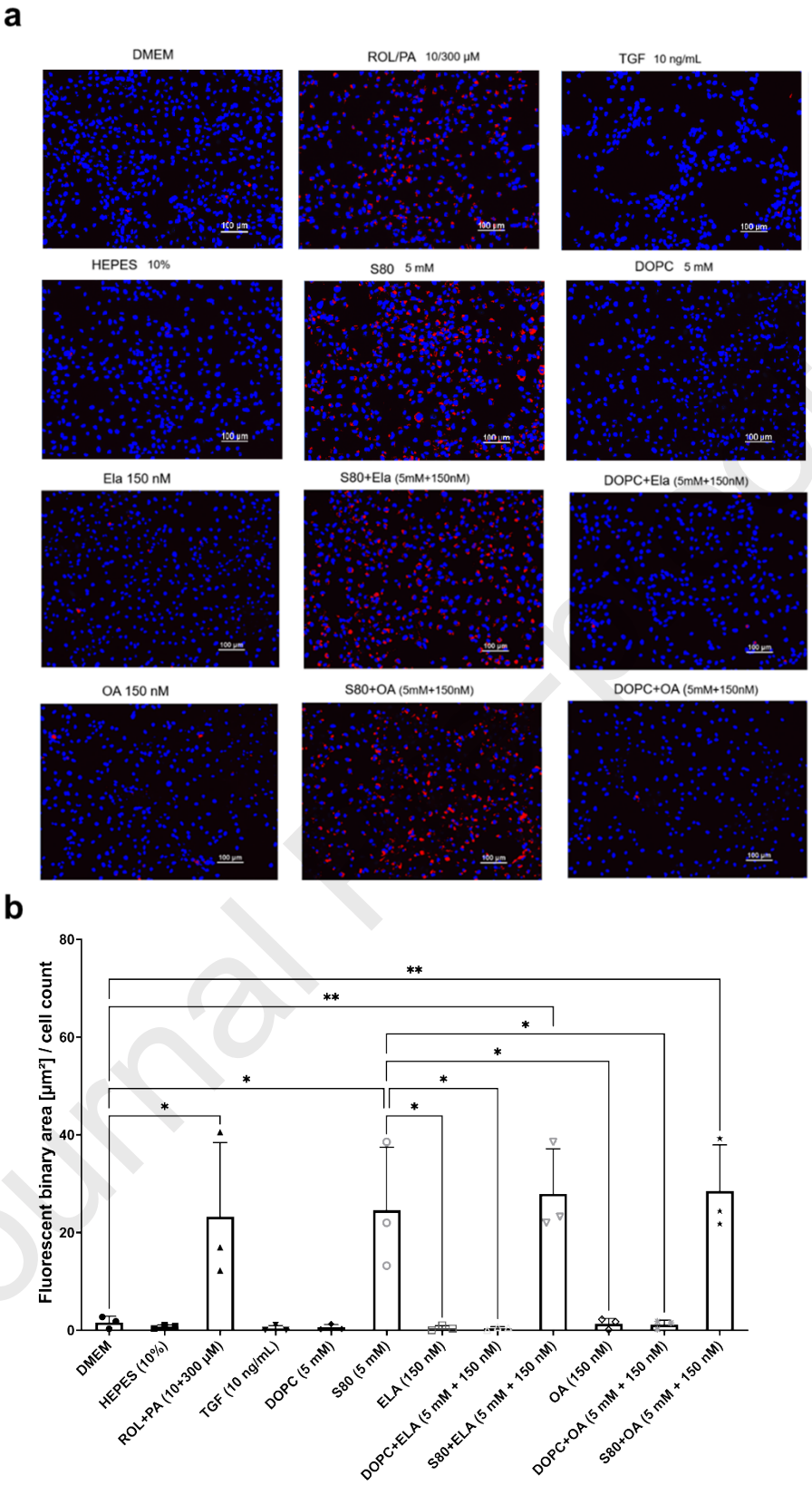

Figure 3. Representative fluorescence images upon ORO staining (visualized as red spots; nuclei stained in blue with DAPI) of differently treated cells (a). Total lipid concentration was 5 mM, Ela or OA concentration 150 nM. Quantitative analysis of stained lipid droplets, whereby the fluorescent area (correlating to a quiescent-like status) was normalized to cell count (b) (mean ± SD, n = 3). PPC-based formulations were used either on the day they were produced or up to 3 days after being kept at 4 °C for the lipids alone, since we had already established their stability.[41] *P* values ($p \leq 0.05$ (*), $p \leq 0.01$ (**)) were determined by one-way ANOVA on ranks and Tukey's multiple comparison. The complete statistical evaluation is available as Table S1.

3.3 Lipidomic analyses of LX-2 cells and EVs

We recently optimized our *in vitro* LX-2 cell model by developing a robust methodological approach that includes the isolation and analysis of EVs [54]. When compared with parental LX-2 cells, EVs have a higher proportion of PC and phosphatidylglycerol (PG) and lower proportion of phosphatidylethanolamine (PE) and phosphatidylinositol (PI) (**Figure S5**). Strongest enriched in EVs are fully saturated species, i.e., PC(palmitic acid (16:0)/16:0), PI(myristic acid (14:0)/16:0), PI(16:0/16:0), PG(stearic acid (18:0)/18:0), and phospholipids containing polyunsaturated fatty acids (PUFAs), i.e., PC(18:0/arachidonic acid (20:4)), PC(18:0/docosapentaenoic acid (22:5)), PC(16:0/docosahexaenoic acid (22:6)), PI(16:0/20:4), PI(palmitoleic acid (16:1)/20:4) (**Figure S6a**), as well as free 20:4 (**Figure S6b**).

Using a targeted phospholipidomics approach, we investigated the impact of S80 and PC(oleic acid (18:1)/18:1) (DOPC) on the phospholipid profile of cells and EVs. Supplementation of S80 substantially increased the levels of the major components PC(16:0/linoleic acid (18:2)) and PC(18:0/18:2) in both systems (**Figure 4a** and **S7**) and elevated the total PC content, reaching significance for EVs (**Figure 4b**). Neither other phospholipid classes than PC nor free fatty acids (FFA) were enriched following treatment with S80 in cells (**Figure S8**). More pronounced were the cellular changes in the relative composition of species throughout lipid classes (**Figure S9-11**), with S80 increasing the availability of free PUFAs relative to saturated fatty acids (**Figure S12**). DOPC also elevated the PC amount of EVs but less pronounced than S80 (**Figure 4b**). The already high proportion of PC(18:1/18:1) in cells was instead hardly further increased by DOPC (**Figure 4a**), and also free 18:1 levels were not raised (**Figure S12**). Despite this apparent lack of cellular availability, PC(18:1/18:1) was incorporated into EVs to a substantial extend (**Figure 4a**).

Our data suggest that 18:2 and 18:3 are released from excess S80 by phospholipases A_2, converted to 20:3, 20:4, 22:5, 22:5, and 22:6 by desaturases and elongases [61], and

incorporated into phospholipids by acyltransferase isoenzymes.[62,63] Along these lines, the increased availability of PUFAs (20:4 > 22:4 > 20:3 > 22:6 > 22:5 > 18:2 > 20:5) in S80-treated cells (**Figure S12**) is associated with a higher proportion of multiple PUFA-containing PE, PI and PG species (**Figure S9-11**). S80 also increased the PUFA ratio of phospholipids in EVs but with a different profile as compared to cells (**Figure S9-11**), and only in EVs, S80 (but not DOPC) elevated the total amount of PE and, by trend, of PI, and PG (**Figure S8**). Thus, PE(16:0/18:2) was strongest upregulated in EVs upon treatment with S80, whereas elongated/desaturated 18:2 metabolites (20:4, 22:4, 22:5, 22:6) were the dominating fatty acids that accumulate in cellular PE (**Figure S9**). As expected from the failure of DOPC to raise free 18:1 levels (**Figure S12**), the proportion of 18:1-derived PE, PI and PG species was hardly elevated or even decreased (**Figure S9-11**).

Treatment with either OA or Ela lowered the content of PG, PI and less PE in LX-2 cells (**Figure S9**) and decreased the abundance of major phospholipid classes, including PC, in LX-2-derived EVs (**Figure 4b** and **S7**), with PC(16:0/18:2) being one of the phospholipid species strongest depleted (**Figure 4a**). Remarkably, S80 and DOPC failed to elevate the PC content in OA- or Ela-treated cells (**Figure 4b**), but compensated for the OA- and Ela-induced drop of PC in EVs (**Figure 4b**) as well as, in case of S80, the depletion of PC(16:0/18:2) in LX-2 cells (**Figure 4a**). The latter was accompanied by an accumulation of PUFA-containing PC species that is characteristic for S80 (**Figure 4a**). Taken together, the PC fatty acid profile of EVs is shaped by the supplemented phospholipid rather than the drug candidate, when the two are combined. Thus, 18:2-containing PC species preferentially increased in EVs upon treatment with S80, and PC(18:1/18:1) was strongest upregulated by addition of DOPC (**Figure 4a**).

OA and Ela also influenced the PE, PI and PG fatty acid composition of LX-2 cells, and both S80 and DOPC further modulated these changes (**Figure S9-S11**). For example, OA and Ela substantially lowered cellular PG(18:1/18:1) levels, which was diminished by co-treatment with S80 (**Figure S12**). The consequences of OA and Ela on the phospholipid fatty acid composition

of EVs were even more diverse, as were the combinatory effects of S80 and DOPC (**Figure S9-S11**). For instance, OA and Ela upregulated the ratio of PE(16:1/22:4), which was prevented by S80 or DOPC, whereas the proportion of other PUFA-containing PE species was hardly affected or even reduced by the combined treatment (**Figure S9**).

Total FFA levels tend to increase in EVs only when cells were co-treated with either S80/OA or ELA/DOPC (**Figure S8**), primarily by upregulating distinct PUFA species, among them 18:2 (**Figure S12**). However, an increase in the PUFA ratio does not (necessarily) elevate the total FFA content in EVs, as can be seen from the co-treatment with S80/Ela, which raised the proportion of free PUFAs (**Figure S12**) without affecting the total FFA concentration (**Figure S8**).

In summary, our lipidomic analysis shows similarities in the phospholipid composition of EVs and the cells they are originating from, but there are also substantial differences, both in the abundance of phospholipid classes as well as in their composition. We further demonstrate that supplementation of specific phospholipids to the parental cells via liposomes allows to adjust the phospholipid composition of EVs. Note that the consequences of exogenous phospholipids on the lipid composition depend on the cellular lipid metabolism and strongly differ between EVs and cells. Marked changes in the EV phospholipid pattern emerge also upon treatment with experimental drugs directed against non-alcoholic fatty liver disease, with supplementation of S80 more than DOPC partially preventing or redirecting the effects.

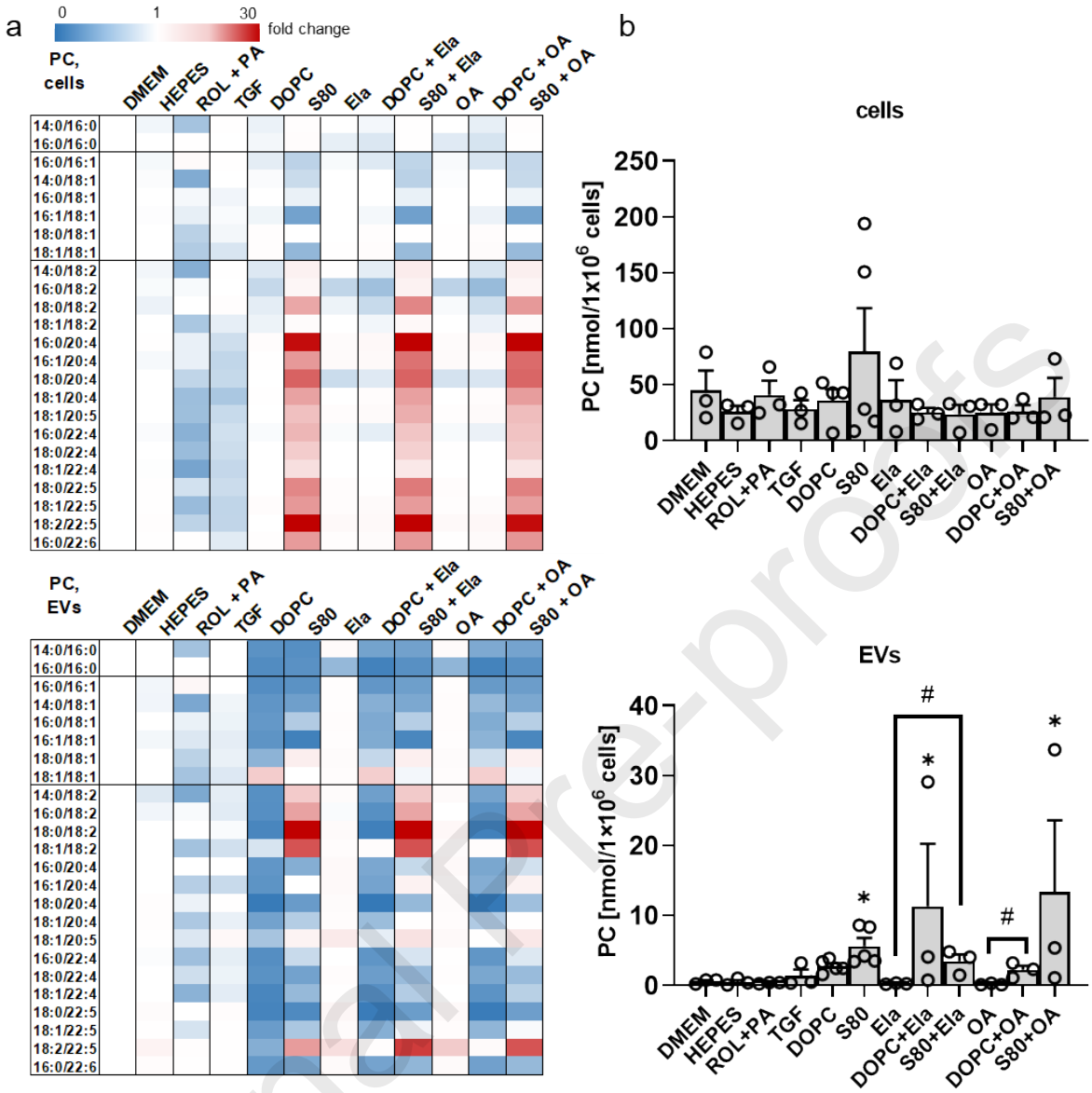

Figure 4. Phosphatidylcholine (PC) content and fatty acid profile of differently treated cells and their EV fractions. Heatmaps showing fold changes in the proportion of individual PC species (calculated as percentage of total PC) relative to the DMEM control (a). Absolute amount of PC as sum of the PC species analyzed (b). Data are presented as means ± S.E.M. of 3 (DMEM, HEPES, ROL+PA, TGF, Ela, DOPC+Ela, S80+Ela, OA, DOPC+OA, S80+OA) or 5 (DOPC, S80) independent experiments. Total lipid concentration for liposomal treatments was 5 mM, Ela or OA concentration 150 nM. $^{\#}P<0.05$, student unpaired *t*-test; $^{*}P<0.05$, mixed-type ANOVA + Dunnett's test with DMEM as control group.

3.4 Detection of EV-associated SPARC after treatment with Ela and OA

To date, studies on Ela and OA focused on their biological activity and therapeutic role played on hepatocytes, their primary target, and little is known on their effect on HSCs. Specifically, how these two active principles may affect the intercellular communication in the HSC-

mediated fibrogenic process and correspondingly protein and lipid composition of EVs was, to our knowledge, never investigated [59].

We previously evaluated the protein profiles of EVs isolated from different HSCs and successfully optimized an immunolabeling protocol for detecting rationally selected proteins on single EVs by f-NTA [54]. SPARC was chosen as a model protein given its known role in wound healing and ECM production, and we observed that its relative abundance associated to EVs varied upon different cell treatments. Here, we used this non-destructive approach to evaluate the performance of OA and Ela, either as free drugs or delivered with drug-loaded PPC-based liposomes, with the aim to explore a possible synergistic effect.

Incubating the parent cells with 150 nM of either Ela or OA caused a 3- and 4-fold increase in the relative amounts of SPARC-positive EVs, which was countered by DOPC, and even more efficiently by S80 (**Figure 5**). It is now also evident that even 150 nM concentrations of Ela and OA elicit a significant response from the HSCs, measurable by analysing their EVs. We could show a deactivation of HSCs' transdifferentiation by S80 as it correlates to SPARC abundance on EVs, thus providing new insights into its mode of action. Moreover, our data provide a putative explanation for the underperforming clinical outcome of the experimental drugs Ela and OA, which is seemingly tied to the relative presence of SPARC on HSC-EVs, warranting further exploration.

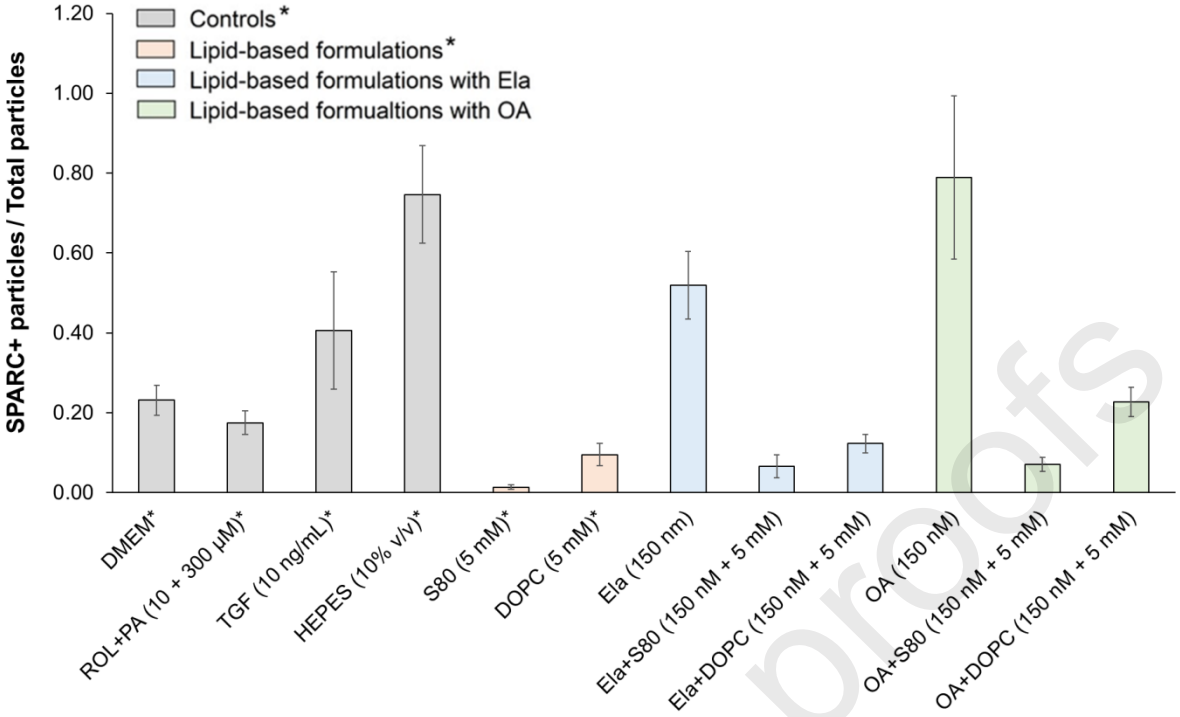

Figure 5. Detection of SPARC via fNTA on EVs isolated from differently treated LX-2 cells (mean ± SD, n = 3). Total lipid concentration for liposomal treatments was 5 mM, Ela or OA concentration 150 nM. Asterisks indicate data sets we have previously published [54] and are reporting here with permission.

4. Conclusion

After establishing the compatibility of Ela and OA with our liposome-production methods we showed that lipid-vesicles could successfully be loaded with Ela and OA. A reliable quantification can be achieved. Lipid vesicles were all monodisperse, around 150 nm in size, and stable at 4 °C for 21 d.

The drugs' effect alone and in combination with PPC-liposomes was explored by ORO/DAPI-staining of cytoplasmic lipid droplets and cell nuclei. There was little toxicity shown in a cell viability assay based on the measurement of mitochondrial dehydrogenase activity up to concentrations of 75 µM.

Any beneficial effect on HSCs of drugs such as OA and Ela on HSCs will have to be determined by screening the functional cell response and including all the known quiescence hallmark for this cell type. However, there is also the possibility that there is no antifibrotic effect to detect from Ela and OA in our *in vitro* model. Both drugs have failed to meet recent expectations in

phase 3 clinical trials [37,38], and it is possible that significant improvements for certain cells in the liver are countered by a fibrogenic response from HSCs. With our analytical tools to evaluate LX-2-EVs [54] we can now offer novel scientific evidence on the effect of Ela and OA on HSCs and derived EVs, and propose these methods for *in vitro* screening of antifibrotic drug candidates.

Indeed, we quantitatively assessed the performance of drugs and anti-fibrotic PPCs, while also providing novel insights into the effects they exert on HSCs, especially for S80, Ela and OA, tracking the presence of SPARC. SPARC-positive EVs are here used to estimate the efficacy of drugs/phospholipids on HSC transdifferentiation that correlates with disease. The increased SPARC presence on HSC-EVs upon drug treatments was substantially mitigated by co-formulation with phospholipids, suggesting that their delivery in PPC-based dosage forms could reignite or potentiate their clinical success. All these protocols and insights should be further tested on primary cells, as well as on *ex vivo* biological fluids from patients and healthy volunteers, possibly extending them to include other candidate biomarkers.

Acknowledgements

The Phospholipid Research Center is kindly acknowledged for the financial support (Grant ID: PLU-2017-056/2-1, AKO-2019-070/2-1). G.F. would like to acknowledge financial support from the NanoMatFutur program from the Federal Ministry of Research and Education (grant number 13XP5029A).

Declaration of competing interests

No private study sponsors had any involvement in the study design, data collection, or interpretation of data presented in this manuscript. P.L. declares the following competing interests: she has consulted Lipoid GmbH and Sanofi-Aventis Deutschland, and received

research grants from Lipoid, Sanofi-Aventis Deutschland and DSM Nutritional Products Ltd. C.Z., A.K., F.W., and G.F. declare no competing interests.

References

[1] S.K. Asrani, H. Devarbhavi, J. Eaton, P.S. Kamath, Burden of liver diseases in the world, J. Hepatol. 70 (2019) 151–171. https://doi.org/10.1016/j.jhep.2018.09.014.

[2] L. Pimpin, H. Cortez-Pinto, F. Negro, E. Corbould, J. V. Lazarus, L. Webber, N. Sheron, Burden of liver disease in Europe: Epidemiology and analysis of risk factors to identify prevention policies, J. Hepatol. 69 (2018) 718–735. https://doi.org/10.1016/j.jhep.2018.05.011.

[3] N. Ndugga, T.G. Lightbourne, K. Javaherian, J. Cabezas, N. Verma, A.S. Barritt, R. Bataller, Disparities between research attention and burden in liver diseases: implications on uneven advances in pharmacological therapies in Europe and the USA, BMJ Open. 7 (2017) e013620. https://doi.org/10.1136/bmjopen-2016-013620.

[4] R.A. Vreman, A.J. Goodell, L.A. Rodriguez, T.C. Porco, R.H. Lustig, J.G. Kahn, Health and economic benefits of reducing sugar intake in the USA, including effects via non-alcoholic fatty liver disease: A microsimulation model, BMJ Open. 7 (2017) e013543. https://doi.org/10.1136/bmjopen-2016-013543.

[5] D.R. LaBrecque, Z. Abbas, F. Anania, P. Ferenci, A.G. Khan, K.-L. Goh, S.S. Hamid, V. Isakov, M. Lizarzabal, M.M. Peñaranda, J.F.R. Ramos, S. Sarin, D. Stimac, A.B.R. Thomson, M. Umar, J. Krabshuis, A. LeMair, World Gastroenterology Organisation Global Guidelines, J. Clin. Gastroenterol. 48 (2014) 467–473. https://doi.org/10.1097/MCG.0000000000000116.

[6] P. Marcellin, B.K. Kutala, Liver diseases: A major, neglected global public health problem requiring urgent actions and large-scale screening, Liver Int. 38 (2018) 2–6.

https://doi.org/10.1111/liv.13682.

[7] H. Hagström, P. Nasr, M. Ekstedt, U. Hammar, P. Stål, R. Hultcrantz, S. Kechagias, Fibrosis stage but not NASH predicts mortality and time to development of severe liver disease in biopsy-proven NAFLD, J. Hepatol. 67 (2017) 1265–1273. https://doi.org/10.1016/j.jhep.2017.07.027.

[8] A. Altamirano-Barrera, B. Barranco-Fragoso, N. Méndez-Sánchez, Management strategies for liver fibrosis, Ann. Hepatol. 16 (2017) 48–56. https://doi.org/10.5604/16652681.1226814.

[9] S. Paul, A.M. Davis, Diagnosis and Management of Nonalcoholic Fatty Liver Disease, JAMA. 320 (2018) 2474. https://doi.org/10.1001/jama.2018.17365.

[10] T.T. Chang, Y.F. Liaw, S.S. Wu, E. Schiff, K.H. Han, C.L. Lai, R. Safadi, S.S. Lee, W. Halota, Z. Goodman, Y.C. Chi, H. Zhang, R. Hindes, U. Iloeje, S. Beebe, B. Kreter, Long-term entecavir therapy results in the reversal of fibrosis/cirrhosis and continued histological improvement in patients with chronic hepatitis B, Hepatology. 52 (2010) 886–893. https://doi.org/10.1002/hep.23785.

[11] A.J. Montano-Loza, R.B. Thandassery, A.J. Czaja, Targeting Hepatic Fibrosis in Autoimmune Hepatitis, Dig. Dis. Sci. 61 (2016) 3118–3139. https://doi.org/10.1007/s10620-016-4254-7.

[12] A.J. Czaja, H.A. Carpenter, Decreased fibrosis during corticosteroid therapy of autoimmune hepatitis, in: J. Hepatol., Elsevier, 2004: pp. 646–652. https://doi.org/10.1016/j.jhep.2004.01.009.

[13] C.L. Bowlus, J.T. Kenney, G. Rice, R. Navarro, Primary Biliary Cholangitis: Medical and Specialty Pharmacy Management Update, J. Manag. Care Spec. Pharm. 22 (2016) S3–S15. https://doi.org/10.18553/jmcp.2016.22.10-a-s.s3.

[14] E. Lefebvre, G. Moyle, R. Reshef, L.P. Richman, M. Thompson, F. Hong, H. Chou, T. Hashiguchi, C. Plato, D. Poulin, T. Richards, H. Yoneyama, H. Jenkins, G. Wolfgang,

S.L. Friedman, Antifibrotic Effects of the Dual CCR2/CCR5 Antagonist Cenicriviroc in Animal Models of Liver and Kidney Fibrosis, PLoS One. 11 (2016) e0158156. https://doi.org/10.1371/journal.pone.0158156.

[15] M. Pedrosa, S. Seyedkazemi, S. Francque, A. Sanyal, M. Rinella, M. Charlton, R. Loomba, V. Ratziu, J. Kochuparampil, L. Fischer, S. Vaidyanathan, Q.M. Anstee, A randomized, double-blind, multicenter, phase 2b study to evaluate the safety and efficacy of a combination of tropifexor and cenicriviroc in patients with nonalcoholic steatohepatitis and liver fibrosis: Study design of the TANDEM trial, Contemp. Clin. Trials. 88 (2020) 105889. https://doi.org/10.1016/j.cct.2019.105889.

[16] Q.M. Anstee, B.A. Neuschwander-Tetri, V.W.-S. Wong, M.F. Abdelmalek, Z.M. Younossi, J. Yuan, M.L. Pecoraro, S. Seyedkazemi, L. Fischer, P. Bedossa, Z. Goodman, N. Alkhouri, F. Tacke, A. Sanyal, Cenicriviroc for the treatment of liver fibrosis in adults with nonalcoholic steatohepatitis: AURORA Phase 3 study design, Contemp. Clin. Trials. 89 (2020) 105922. https://doi.org/10.1016/j.cct.2019.105922.

[17] D.C. Tully, P. V. Rucker, D. Chianelli, J. Williams, A. Vidal, P.B. Alper, D. Mutnick, B. Bursulaya, J. Schmeits, X. Wu, D. Bao, J. Zoll, Y. Kim, T. Groessl, P. McNamara, H.M. Seidel, V. Molteni, B. Liu, A. Phimister, S.B. Joseph, B. Laffitte, Discovery of Tropifexor (LJN452), a Highly Potent Non-bile Acid FXR Agonist for the Treatment of Cholestatic Liver Diseases and Nonalcoholic Steatohepatitis (NASH), J. Med. Chem. 60 (2017) 9960–9973. https://doi.org/10.1021/acs.jmedchem.7b00907.

[18] Y. Sumida, M. Yoneda, Current and future pharmacological therapies for NAFLD/NASH, J. Gastroenterol. 53 (2018) 362–376. https://doi.org/10.1007/s00535-017-1415-1.

[19] V. Ratziu, Novel Pharmacotherapy Options for NASH, Dig. Dis. Sci. 61 (2016) 1398–1405. https://doi.org/10.1007/s10620-016-4128-z.

[20] S.A. Townsend, P.N. Newsome, Non-alcoholic fatty liver disease in 2016, Br. Med. Bull.

119 (2016) 143–156. https://doi.org/10.1093/bmb/ldw031.

[21] H. Perazzo, J. Dufour, The therapeutic landscape of non-alcoholic steatohepatitis, Liver Int. 37 (2017) 634–647. https://doi.org/10.1111/liv.13270.

[22] B.A. Neuschwander-Tetri, R. Loomba, A.J. Sanyal, J.E. Lavine, M.L. Van Natta, M.F. Abdelmalek, N. Chalasani, S. Dasarathy, A.M. Diehl, B. Hameed, K. V. Kowdley, A. McCullough, N. Terrault, J.M. Clark, J. Tonascia, E.M. Brunt, D.E. Kleiner, E. Doo, Farnesoid X nuclear receptor ligand obeticholic acid for non-cirrhotic, non-alcoholic steatohepatitis (FLINT): a multicentre, randomised, placebo-controlled trial, Lancet. 385 (2015) 956–965. https://doi.org/10.1016/S0140-6736(14)61933-4.

[23] E. Gore, E. Bigaeva, A. Oldenburger, Y.J.M. Jansen, D. Schuppan, M. Boersema, J.F. Rippmann, A. Broermann, P. Olinga, Investigating fibrosis and inflammation in an ex vivo NASH murine model, Am. J. Physiol. Liver Physiol. 318 (2020) G336–G351. https://doi.org/10.1152/ajpgi.00209.2019.

[24] M.J. Westerouen Van Meeteren, J.P.H. Drenth, E.T.T.L. Tjwa, Elafibranor: a potential drug for the treatment of nonalcoholic steatohepatitis (NASH), Expert Opin. Investig. Drugs. 29 (2020) 117–123. https://doi.org/10.1080/13543784.2020.1668375.

[25] V. Ratziu et al., Elafibranor, an Agonist of the Peroxisome Proliferator-Activated Receptor-α and -δ, Induces Resolution of Nonalcoholic Steatohepatitis Without Fibrosis Worsening, Gastroenterology. 150 (2016) 1147-1159.e5. https://doi.org/10.1053/j.gastro.2016.01.038.

[26] K.S. Tølbøl, M.N.B. Kristiansen, H.H. Hansen, S.S. Veidal, K.T.G. Rigbolt, M.P. Gillum, J. Jelsing, N. Vrang, M. Feigh, Metabolic and hepatic effects of liraglutide, obeticholic acid and elafibranor in diet-induced obese mouse models of biopsy-confirmed nonalcoholic steatohepatitis, World J. Gastroenterol. 24 (2018) 179–194. https://doi.org/10.3748/wjg.v24.i2.179.

[27] J. Zhou, N. Huang, Y. Guo, S. Cui, C. Ge, Q. He, X. Pan, G. Wang, H. Wang, H. Hao,

Combined obeticholic acid and apoptosis inhibitor treatment alleviates liver fibrosis, Acta Pharm. Sin. B. 9 (2019) 526–536. https://doi.org/10.1016/j.apsb.2018.11.004.

[28] J.D. Roth, S.S. Veidal, L.K.D. Fensholdt, K.T.G. Rigbolt, R. Papazyan, J.C. Nielsen, M. Feigh, N. Vrang, M. Young, J. Jelsing, L. Adorini, H.H. Hansen, Combined obeticholic acid and elafibranor treatment promotes additive liver histological improvements in a diet-induced ob/ob mouse model of biopsy-confirmed NASH, Sci. Rep. 9 (2019) 1–13. https://doi.org/10.1038/s41598-019-45178-z.

[29] A. Christofides, E. Konstantinidou, C. Jani, V.A. Boussiotis, The role of peroxisome proliferator-activated receptors (PPAR) in immune responses, Metabolism. 114 (2021) 154338. https://doi.org/10.1016/j.metabol.2020.154338.

[30] H. Gim, Y.-S. Choi, H. Li, Y.-J. Kim, J.-H. Ryu, R. Jeon, Identification of a Novel PPAR-γ Agonist through a Scaffold Tuning Approach, Int. J. Mol. Sci. 19 (2018) 3032. https://doi.org/10.3390/ijms19103032.

[31] B. Staels, J.C. Fruchart, Therapeutic roles of peroxisome proliferator-activated receptor agonists, Diabetes. 54 (2005) 2460–2470. https://doi.org/10.2337/diabetes.54.8.2460.

[32] S.M. Smith, A.H. Pegram, Obeticholic Acid, J. Pharm. Technol. 33 (2017) 66–71. https://doi.org/10.1177/8755122516687122.

[33] R. Pellicciari, S. Fiorucci, E. Camaioni, C. Clerici, G. Costantino, P.R. Maloney, A. Morelli, D.J. Parks, T.M. Willson, 6α-ethyl-chenodeoxycholic acid (6-ECDCA), a potent and selective FXR agonist endowed with anticholestatic activity, J. Med. Chem. 45 (2002) 3569–3572. https://doi.org/10.1021/jm025529g.

[34] S. Fiorucci, C. Clerici, E. Antonelli, S. Orlandi, B. Goodwin, B.M. Sadeghpour, G. Sabatino, G. Russo, D. Castellani, T.M. Willson, M. Pruzanski, R. Pellicciari, A. Morelli, Protective effects of 6-ethyl chenodeoxycholic acid, a farnesoid x receptor ligand, in estrogen-induced cholestasis, J. Pharmacol. Exp. Ther. 313 (2005) 604–612. https://doi.org/10.1124/jpet.104.079665.

[35] Y.-Y. Fan, W. Ding, C. Zhang, L. Fu, D.-X. Xu, X. Chen, Obeticholic acid prevents carbon tetrachloride-induced liver fibrosis through interaction between farnesoid X receptor and Smad3, Int. Immunopharmacol. 77 (2019) 105911. https://doi.org/10.1016/j.intimp.2019.105911.

[36] L. Verbeke, I. Mannaerts, R. Schierwagen, O. Govaere, S. Klein, I. Vander Elst, P. Windmolders, R. Farre, M. Wenes, M. Mazzone, F. Nevens, L.A. van Grunsven, J. Trebicka, W. Laleman, FXR agonist obeticholic acid reduces hepatic inflammation and fibrosis in a rat model of toxic cirrhosis, Sci. Rep. 6 (2016) 33453. https://doi.org/10.1038/srep33453.

[37] GENFIT, Press Release : Provides Initial Update on Corporate Strategy, Press Release. (2020).

[38] Intercept, Intercept receives complete response letter from FDA for obeticholic acid for the treatment of fibrosis due to NASH., Press Release. (2020).

[39] K.-J. Gundermann, A. Kuenker, E. Kuntz, M. Droździk, Activity of essential phospholipids (EPL) from soybean in liver diseases, Pharmacol. Reports. 63 (2011) 643–659. https://doi.org/10.1016/S1734-1140(11)70576-X.

[40] A.I.M. Dajani, A.M. Abu Hammour, M.A. Zakaria, M.R. Al Jaberi, M.A. Nounou, A.I.M. Semrin, Essential phospholipids as a supportive adjunct in the management of patients with NAFLD, Arab J. Gastroenterol. 16 (2015) 99–104. https://doi.org/10.1016/j.ajg.2015.09.001.

[41] G. Valentino, C. Zivko, F. Weber, L. Brülisauer, P. Luciani, Synergy of Phospholipid—Drug Formulations Significantly Deactivates Profibrogenic Human Hepatic Stellate Cells, Pharmaceutics. 11 (2019) 676. https://doi.org/10.3390/pharmaceutics11120676.

[42] S.L. Friedman, Mechanisms of Hepatic Fibrogenesis, Gastroenterology. 134 (2008) 1655–1669. https://doi.org/10.1053/j.gastro.2008.03.003.

[43] A. Pellicoro, P. Ramachandran, J.P. Iredale, J.A. Fallowfield, Liver fibrosis and repair:

immune regulation of wound healing in a solid organ, Nat. Rev. Immunol. 14 (2014) 181–194. https://doi.org/10.1038/nri3623.

[44] M. Parola, M. Pinzani, Liver fibrosis: Pathophysiology, pathogenetic targets and clinical issues, Mol. Aspects Med. 65 (2019) 37–55. https://doi.org/10.1016/j.mam.2018.09.002.

[45] J.Y.-K. Cheng, G.L.-H. Wong, Advances in the diagnosis and treatment of liver fibrosis, Hepatoma Res. 3 (2017) 156. https://doi.org/10.20517/2394-5079.2017.27.

[46] K.W. Witwer, C. Théry, Extracellular vesicles or exosomes? On primacy, precision, and popularity influencing a choice of nomenclature, J. Extracell. Vesicles. 8 (2019) 1648167. https://doi.org/10.1080/20013078.2019.1648167.

[47] C. Théry et al., Minimal information for studies of extracellular vesicles 2018 (MISEV2018): a position statement of the International Society for Extracellular Vesicles and update of the MISEV2014 guidelines, J. Extracell. Vesicles. 7 (2018) 1535750. https://doi.org/10.1080/20013078.2018.1535750.

[48] Y. Kawamura, Y. Yamamoto, T.A. Sato, T. Ochiya, Extracellular vesicles as trans-genomic agents: Emerging roles in disease and evolution, Cancer Sci. 108 (2017) 824–830. https://doi.org/10.1111/cas.13222.

[49] R. Ono, Y. Yasuhiko, K. Aisaki, S. Kitajima, J. Kanno, Y. Hirabayashi, Exosome-mediated horizontal gene transfer occurs in double-strand break repair during genome editing, Commun. Biol. 2 (2019) 57. https://doi.org/10.1038/s42003-019-0300-2.

[50] I.K. Herrmann, M.J.A. Wood, G. Fuhrmann, Extracellular vesicles as a next-generation drug delivery platform, Nat. Nanotechnol. 2021 167. 16 (2021) 748–759. https://doi.org/10.1038/s41565-021-00931-2.

[51] Z. Zhao, J. Fan, Y.M.S. Hsu, C.J. Lyon, B. Ning, T.Y. Hu, Extracellular vesicles as cancer liquid biopsies: From discovery, validation, to clinical application, Lab Chip. 19 (2019) 1114–1140. https://doi.org/10.1039/c8lc01123k.

[52] S. Urban, T. Mocan, H. Sänger, V. Lukacs-Kornek, M. Kornek, Extracellular Vesicles

in Liver Diseases: Diagnostic, Prognostic, and Therapeutic Application, Semin. Liver Dis. 39 (2019) 070–077. https://doi.org/10.1055/s-0038-1676122.

[53] L. Barile, G. Vassalli, Exosomes: Therapy delivery tools and biomarkers of diseases, Pharmacol. Ther. 174 (2017) 63–78. https://doi.org/10.1016/J.PHARMTHERA.2017.02.020.

[54] C. Zivko, K. Fuhrmann, G. Fuhrmann, P. Luciani, Tracking matricellular protein SPARC in extracellular vesicles as a non-destructive method to evaluate lipid-based antifibrotic treatments, Commun. Biol. 5 (2022) 1155. https://doi.org/10.1038/s42003-022-04123-z.

[55] P. Königshofer, K. Brusilovskaya, O. Petrenko, B.S. Hofer, P. Schwabl, M. Trauner, T. Reiberger, Nuclear receptors in liver fibrosis, Biochim. Biophys. Acta - Mol. Basis Dis. 1867 (2021) 166235. https://doi.org/10.1016/j.bbadis.2021.166235.

[56] F. Weber, L. Rahnfeld, P. Luciani, Analytical profiling and stability evaluation of liposomal drug delivery systems: A rapid UHPLC-CAD-based approach for phospholipids in research and quality control, Talanta. 220 (2020) 121320. https://doi.org/10.1016/j.talanta.2020.121320.

[57] A. Koeberle, H. Shindou, S.C. Koeberle, S.A. Laufer, T. Shimizu, O. Werz, Arachidonoyl-phosphatidylcholine oscillates during the cell cycle and counteracts proliferation by suppressing Akt membrane binding, Proc. Natl. Acad. Sci. U. S. A. 110 (2013) 2546–2551. https://doi.org/10.1073/pnas.1216182110.

[58] A. Koeberle, C. Pergola, H. Shindou, S.C. Koeberle, T. Shimizu, S.A. Laufer, O. Werz, Role of p38 mitogen-activated protein kinase in linking stearoyl-CoA desaturase-1 activity with endoplasmic reticulum homeostasis, FASEB J. 29 (2015) 2439–2449. https://doi.org/10.1096/fj.14-268474.

[59] A. Zisser, D.H. Ipsen, P. Tveden-Nyborg, Hepatic Stellate Cell Activation and Inactivation in NASH-Fibrosis—Roles as Putative Treatment Targets?, Biomedicines. 9 (2021) 365. https://doi.org/10.3390/biomedicines9040365.

[60] B. Kong, J.P. Luyendyk, O. Tawfik, G.L. Guo, Farnesoid X Receptor Deficiency Induces Nonalcoholic Steatohepatitis in Low-Density Lipoprotein Receptor-Knockout Mice Fed a High-Fat Diet, J. Pharmacol. Exp. Ther. 328 (2009) 116–122. https://doi.org/10.1124/jpet.108.144600.

[61] R.K. Saini, Y.S. Keum, Omega-3 and omega-6 polyunsaturated fatty acids: Dietary sources, metabolism, and significance — A review, Life Sci. 203 (2018) 255–267. https://doi.org/10.1016/j.lfs.2018.04.049.

[62] H. Sprecher, D.L. Luthria, B.S. Mohammed, S.P. Baykousheva, Reevaluation of the pathways for the biosynthesis of polyunsaturated fatty acids., J. Lipid Res. 36 (1995) 2471–2477. https://doi.org/10.1016/S0022-2275(20)41084-3.

[63] H. Shindou, D. Hishikawa, T. Harayama, M. Eto, T. Shimizu, Generation of membrane diversity by lysophospholipid acyltransferases, J. Biochem. 154 (2013) 21–28. https://doi.org/10.1093/jb/mvt048.

Cristina Zivko, Finja Witt, Andreas Koeberle, Gregor Fuhrmann, Paola Luciani**

Formulating elafibranor and obeticholic acid with phospholipids decreases drug-induced association of SPARC to extracellular vesicles from LX-2 human hepatic stellate cells

Extracellular vesicles (EVs) are important mediator of intercellular communication. EVs from hepatic stellate cells, the main collagen-producing cells during hepatic fibrogenesis, were thoroughly analyzed upon different lipid-based treatments. This research shed light on the possible action of two experimental drugs, elafibranor and obeticholic acid, on HSCs and potentially paves the way to non-invasive methods for the evaluation of liver fibrosis and its therapy.

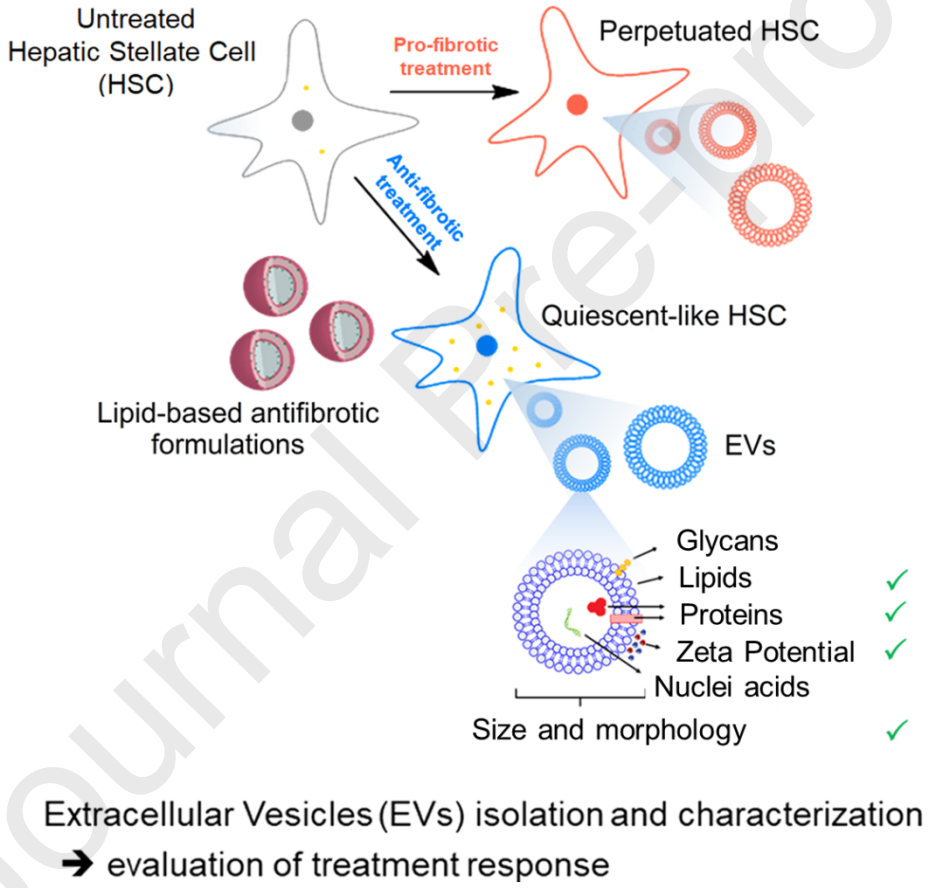

Supporting information

Formulating elafibranor and obeticholic acid with phospholipids decreases drug-induced association of SPARC to extracellular vesicles from LX-2 human hepatic stellate cells

Cristina Zivko, Finja Witt, Andreas Koeberle, Gregor Fuhrmann, Paola Luciani**

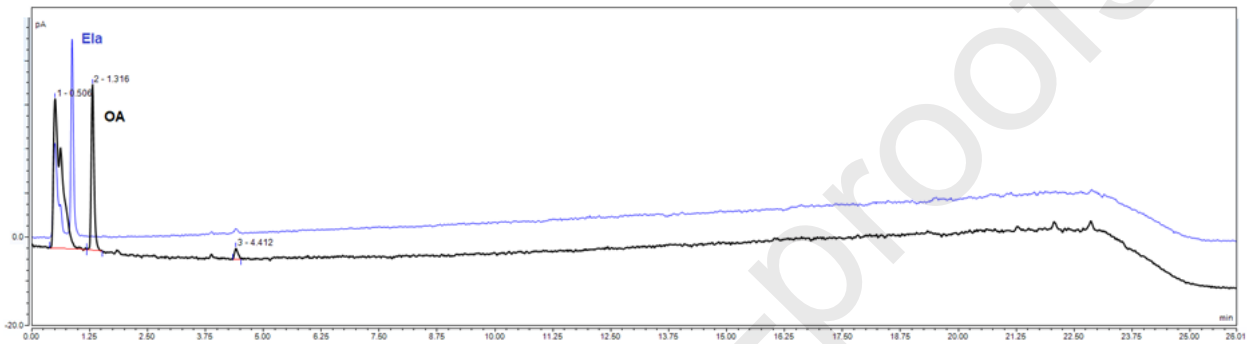

Figure S1. Representative chromatograms for Ela and OA with the same method as with as detected with the CAD (t_R Ela: 1.036 min; t_R OA: 1.308 min). The ghost peaks along the baseline were present in blank samples too, as well as in HPLC runs of other users.

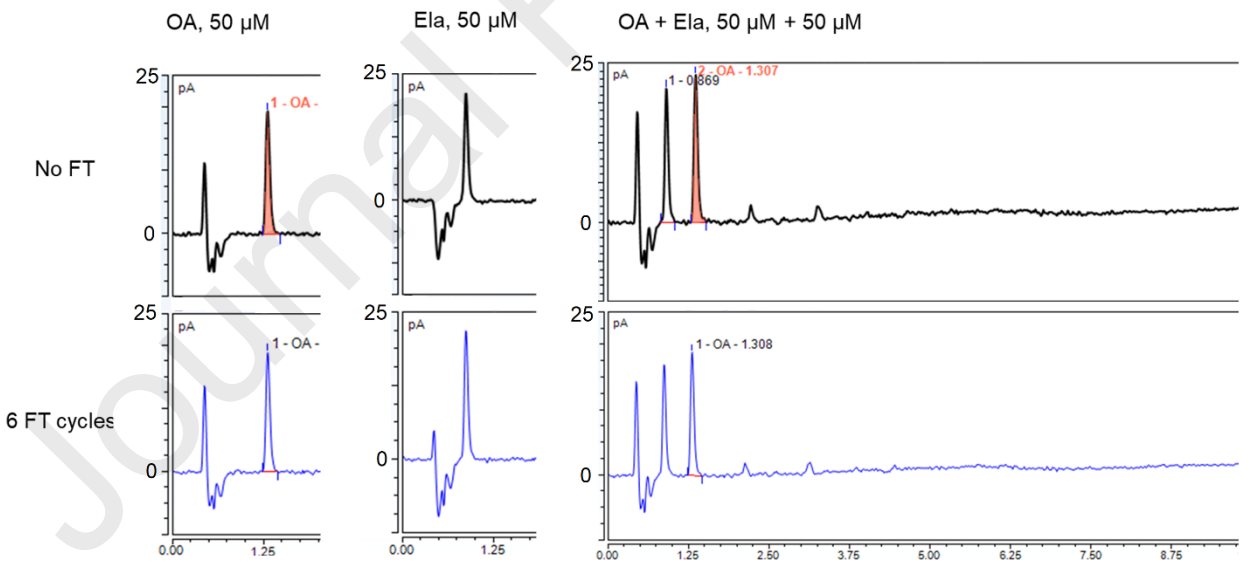

Figure S2. Representative chromatograms of Ela and OA before and after undergoing 6 freeze-thaw (FT) cycles, either separately or in the same sample.

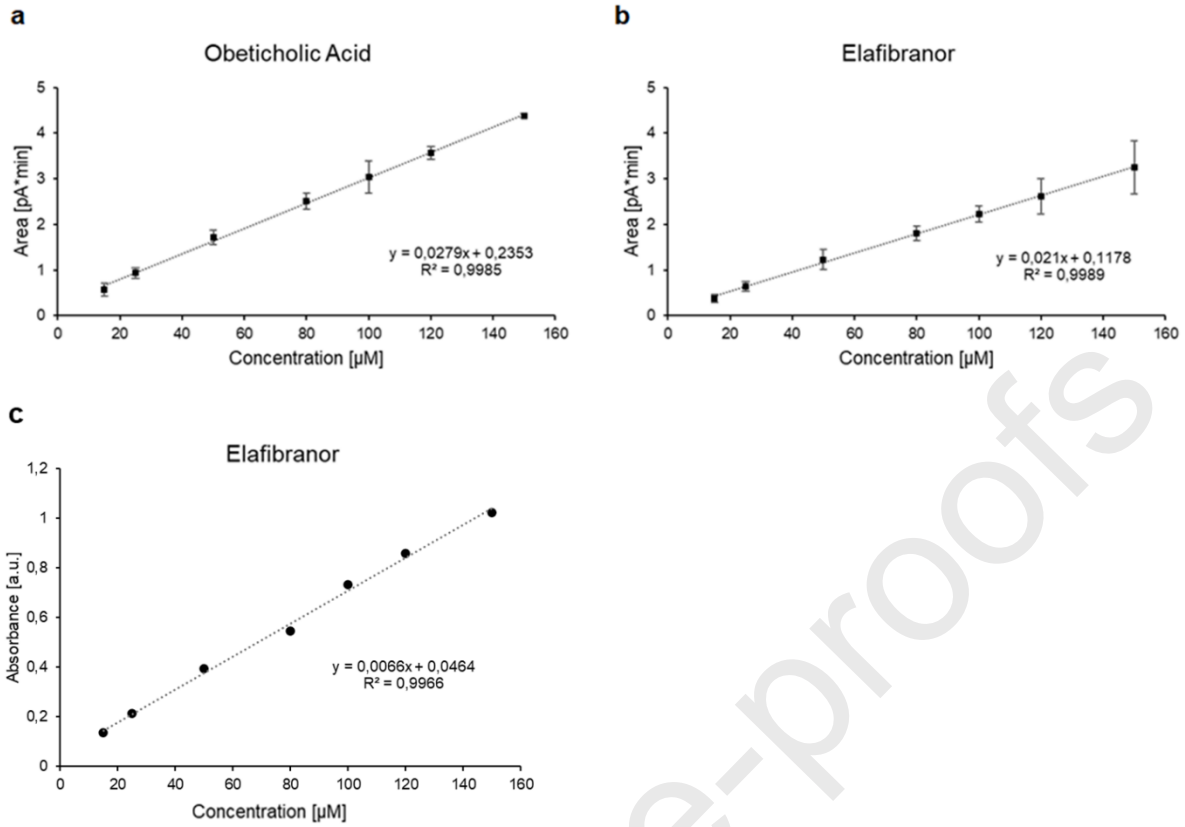

Figure S3. Calibrations curves of OA (a) and Ela (b) by HPLC. When calculated using the standard deviations of the lowest concentration,[51] the lower detection and quantification limits (LOD, LOQ) for OA were 16 and 52 µM, respectively, 13 and 42 µM for Ela. Alternatively, basing the calculation on the signal-to-noise ratio, LOD for both drugs was 3-5 µM and LOQ 15 µM. Calibration curve for Ela obtain with a plate reader (c, λ_{abs} = 358 nm). Mean ± SD, n = 3.

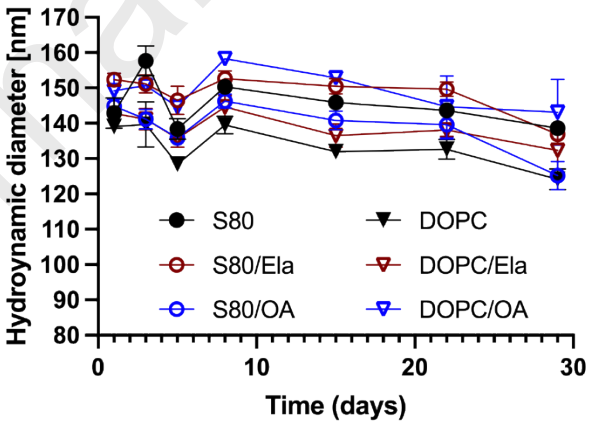

Figure S4. Hydrodynamic diameter of DOPC and S80 liposomes, formulated with and without drugs (OA and Ela), measured over 28 days. The samples were stored at 4 °C.

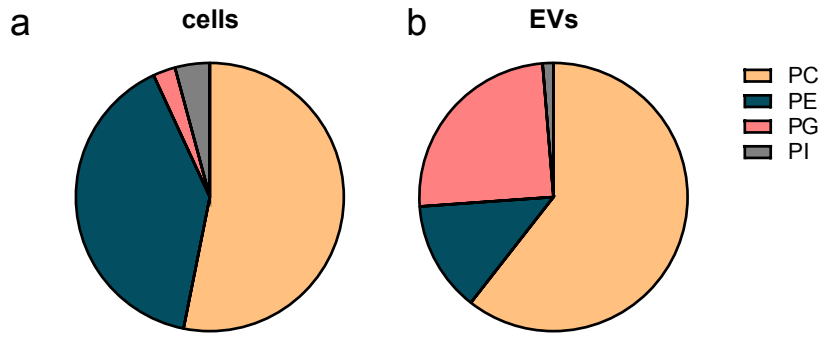

Figure S5. Phospholipid composition of LX-2 cells (a) in comparison to EVs isolated from the cell culture medium (b). The sum of the absolute amounts of all PC, PE, PG, and PI species analyzed is defined as 100% and refers to the DMEM control group. Data are presented as means of 3 independent experiments.

a

0 1 5 fold change

	PC			PE			PG			PI		
	mean	±	SEM	mean	±	SEM	mean	±	SEM	mean	±	SEM
14:0/16:0	6.5	±	0.2	0.6	±	0.01	0.2	±	0.1	0.01	±	0.002
16:0/16:0	16.9	±	1.3	1.4	±	0.1	0.9	±	0.4	0.2	±	0.01
18:0/18:0							0.3	±	0.1			
16:0/16:1	18.5	±	0.6	5.4	±	0.2	1.0	±	0.4	1.3	±	0.1
14:0/18:1	3.0	±	0.1	1.1	±	0.1	0.2	±	0.1	0.2	±	0.02
16:0/18:1	16.2	±	0.1	10.7	±	0.1	4.8	±	2.0	3.1	±	0.1
16:1/18:1	11.5	±	0.4	8.8	±	0.5	1.6	±	0.6	6.7	±	0.2
18:0/18:1	3.0	±	0.1	22.5	±	0.4	10.4	±	4.5	9.8	±	0.6
18:1/18:1	16.6	±	0.2	37.1	±	0.9	76.2	±	9.9	18.0	±	0.9
14:0/18:2	0.5	±	0.02									
16:0/18:2	3.9	±	0.1	1.2	±	0.04	0.2	±	0.1	0.9	±	0.02
18:0/18:2	0.1	±	0.002	2.5	±	0.05	0.9	±	0.4	2.5	±	0.2
18:1/18:2	2.7	±	0.1	1.7	±	0.1	3.2	±	1.3	2.5	±	0.2
16:0/20:3				0.6	±	0.02				2.0	±	0.01
18:0/20:3										40.0	±	1.4
18:1/20:3										8.0	±	0.5
16:0/20:4	0.1	±	0.01	0.5	±	0.03	0.03	±	0.01	0.3	±	0.003
16:1/20:4	0.1	±	0.004	0.1	±	0.004				0.03	±	0.003
18:0/20:4	0.1	±	0.0003	3.0	±	0.1	0.04	±	0.02	3.6	±	0.2
18:1/20:4	0.2	±	0.01	1.1	±	0.05				0.9	±	0.1
18:1/20:5	0.005	±	0.0003									
16:0/22:4	0.1	±	0.001	0.1	±	0.0005						
16:1/22:4				0.01	±	0.0004						
18:0/22:4	0.03	±	0.001	0.7	±	0.02						
18:1/22:4	0.1	±	0.001	0.4	±	0.01						
16:0/22:5				0.04	±	0.001						
18:0/22:5	0.003	±	0.0002	0.3	±	0.01						
18:1/22:5	0.01	±	0.001	0.1	±	0.003						
18:2/22:5	0.001	±	0.0002									
16:0/22:6	0.03	±	0.002	0.1	±	0.01						

b

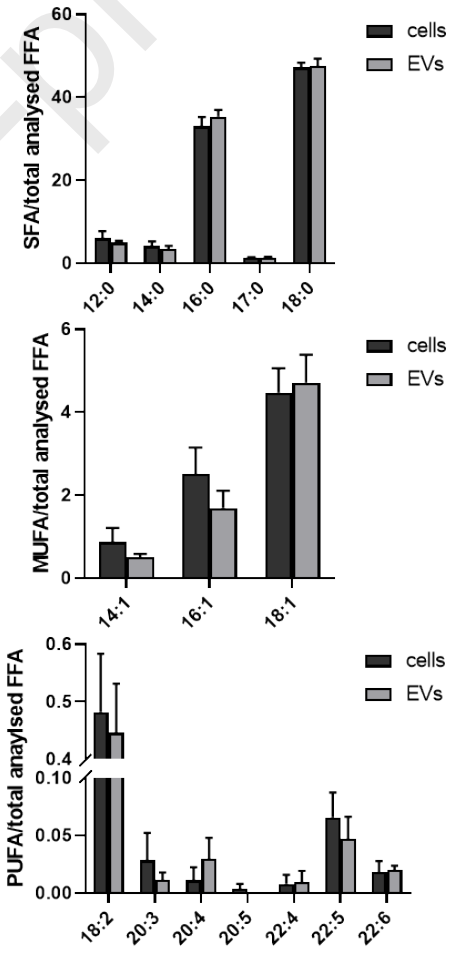

Figure S6. Differences in the free fatty acid composition and phospholipid fatty acid profile of LX-2 cells and their EV fractions. (a) Values indicate the proportion of individual PC, PE, PG, and PI species in DMEM-treated LX-2 cells. Data are given as percentage of the total signal intensity of the respective phospholipid subclass (100%) in LX-2 cells as means ± S.E.M. from 3 independent experiments. The color scale expresses fold changes of the phospholipid proportion in EVs relative to cells. (b) Proportion of individual FFA in DMEM-treated cells and their EV fraction, calculated as percentage of total FFA and subdivided into saturated fatty acid (SFA), monounsaturated fatty acids (MUFAs), and PUFAs. Paired *t*-test of logarithmized values. Data are presented as means + S.E.M. from 3 independent experiments.

0 1 30 fold change

PC, cells	DMEM			HEPES			ROL+PA			TGF			DOPC			S80			Ela			DOPC+Ela			S80+Ela			OA			DOPC+OA			S80+OA		
	mean	±	SEM	mean	±	SEM	mean	±	SEM	mean	±	SEM	mean	±	SEM	mean	±	SEM	mean	±	SEM	mean	±	SEM	mean	±	SEM	mean	±	SEM	mean	±	SEM	mean	±	SEM
14:0/16:0	6.5	±	0.2	6.1	±	0.1	3.7	±	0.3	7.3	±	0.1	5.9	±	0.1	8.2	±	0.5	6.7	±	0.05	6.2	±	0.1	7.7	±	0.6	6.6	±	0.1	5.8	±	0.2	8.2	±	0.2
16:0/16:0	16.9	±	1.3	17.1	±	1.1	20.4	±	2.0	18.4	±	1.9	15.9	±	0.9	23.2	±	1.9	15.0	±	0.1	14.0	±	0.05	19.4	±	0.4	14.4	±	0.5	13.6	±	0.6	19.6	±	0.6
16:0/16:1	18.5	±	0.6	17.7	±	0.3	30.5	±	1.1	21.1	±	0.2	16.2	±	0.6	12.6	±	0.9	17.9	±	0.1	15.7	±	0.2	12.9	±	0.4	17.9	±	0.1	15.1	±	0.8	13.3	±	0.2
14:0/18:1	3.0	±	0.1	2.9	±	0.1	1.2	±	0.1	3.0	±	0.2	2.9	±	0.1	2.2	±	0.1	3.0	±	0.1	3.2	±	0.1	2.0	±	0.2	2.9	±	0.1	3.0	±	0.2	2.1	±	0.1
16:0/18:1	16.2	±	0.1	16.5	±	0.2	15.5	±	0.6	15.1	±	0.4	17.1	±	0.4	14.6	±	0.3	16.6	±	0.3	17.1	±	0.2	14.6	±	0.2	16.6	±	0.2	17.3	±	0.9	15.0	±	0.3
16:1/18:1	11.5	±	0.4	11.5	±	0.3	10.2	±	0.5	11.2	±	0.4	10.7	±	0.3	3.8	±	0.2	11.6	±	0.3	11.0	±	0.2	3.6	±	0.3	11.6	±	0.3	10.5	±	0.8	3.9	±	0.2
18:0/18:1	3.0	±	0.1	3.2	±	0.05	2.0	±	0.1	2.8	±	0.3	3.7	±	0.1	3.1	±	0.2	3.1	±	0.1	3.9	±	0.1	3.4	±	0.1	3.4	±	0.05	4.1	±	0.1	3.5	±	0.1
18:1/18:1	16.6	±	0.2	17.3	±	0.4	10.4	±	1.3	13.6	±	0.7	21.0	±	1.0	8.0	±	0.3	19.1	±	0.4	23.0	±	0.5	8.5	±	0.2	19.7	±	0.2	24.8	±	0.8	8.4	±	0.2
14:0/18:2	0.5	±	0.02	0.4	±	0.02	0.2	±	0.02	0.6	±	0.05	0.4	±	0.03	1.3	±	0.1	0.6	±	0.03	0.4	±	0.01	1.5	±	0.2	0.6	±	0.03	0.4	±	0.04	1.4	±	0.1
16:0/18:2	3.9	±	0.1	3.8	±	0.1	3.8	±	0.02	4.0	±	0.1	2.8	±	0.3	8.2	±	0.4	2.7	±	0.1	2.1	±	0.04	9.8	±	1.4	2.6	±	0.1	2.0	±	0.1	8.7	±	0.9
18:0/18:2	0.1	±	0.002	0.1	±	0.01	0.1	±	0.004	0.2	±	0.04	0.1	±	0.01	1.5	±	0.1	0.1	±	0.01	0.1	±	0.01	2.0	±	0.3	0.1	±	0.002	0.1	±	0.003	1.7	±	0.2
18:1/18:2	2.7	±	0.1	2.8	±	0.2	1.6	±	0.2	2.4	±	0.2	2.4	±	0.1	4.0	±	0.2	2.8	±	0.1	2.5	±	0.03	4.9	±	0.8	2.8	±	0.1	2.4	±	0.1	4.3	±	0.5
16:0/20:4	0.1	±	0.01	0.2	±	0.005	0.1	±	0.01	0.1	±	0.01	0.2	±	0.02	3.9	±	0.2	0.2	±	0.01	0.2	±	0.003	4.1	±	0.2	0.2	±	0.01	0.3	±	0.01	4.2	±	0.1
16:1/20:4	0.1	±	0.004	0.05	±	0.002	0.04	±	0.002	0.04	±	0.003	0.1	±	0.01	0.6	±	0.1	0.1	±	0.01	0.1	±	0.004	0.9	±	0.1	0.1	±	0.01	0.1	±	0.01	0.9	±	0.04
18:0/20:4	0.1	±	0.0003	0.1	±	0.002	0.04	±	0.001	0.04	±	0.01	0.1	±	0.002	1.0	±	0.04	0.04	±	0.001	0.04	±	0.001	1.0	±	0.04	0.04	±	0.001	0.04	±	0.002	1.0	±	0.03
18:1/20:4	0.2	±	0.01	0.2	±	0.01	0.1	±	0.01	0.1	±	0.004	0.2	±	0.01	2.1	±	0.1	0.2	±	0.01	0.2	±	0.01	2.1	±	0.1	0.2	±	0.01	0.2	±	0.02	2.2	±	0.1
18:1/20:5	0.005	±	0.0003	0.005	±	0.001	0.003	±	0.0003	0.003	±	0.0003	0.01	±	0.001	0.04	±	0.003	0.01	±	0.001	0.01	±	0.001	0.05	±	0.01	0.01	±	0.001	0.01	±	0.002	0.04	±	0.001
16:0/22:4	0.1	±	0.001	0.1	±	0.003	0.03	±	0.0002	0.1	±	0.001	0.1	±	0.001	0.7	±	0.05	0.1	±	0.002	0.1	±	0.001	0.6	±	0.1	0.1	±	0.002	0.1	±	0.004	0.6	±	0.02
18:0/22:4	0.03	±	0.001	0.03	±	0.001	0.02	±	0.001	0.02	±	0.001	0.03	±	0.002	0.2	±	0.02	0.03	±	0.001	0.03	±	0.001	0.2	±	0.02	0.03	±	0.002	0.03	±	0.001	0.2	±	0.01
18:1/22:4	0.1	±	0.001	0.1	±	0.001	0.02	±	0.001	0.05	±	0.002	0.1	±	0.002	0.3	±	0.02	0.1	±	0.002	0.1	±	0.0005	0.2	±	0.02	0.1	±	0.002	0.1	±	0.002	0.3	±	0.01
18:0/22:5	0.003	±	0.0002	0.003	±	0.0002	0.002	±	0.0003	0.002	±	0.0001	0.003	±	0.0003	0.04	±	0.002	0.004	±	0.0001	0.003	±	0.0004	0.04	±	0.002	0.004	±	0.0004	0.003	±	0.0003	0.04	±	0.001
18:1/22:5	0.01	±	0.001	0.01	±	0.001	0.004	±	0.001	0.01	±	0.0004	0.01	±	0.001	0.1	±	0.005	0.01	±	0.001	0.01	±	0.001	0.1	±	0.01	0.01	±	0.001	0.01	±	0.001	0.1	±	0.01
18:2/22:5	0.001	±	0.0002	0.001	±	0.0002	0.001	±	0.0001	0.001	±	0.0002	0.001	±	0.0001	0.03	±	0.003	0.002	±	0.001	0.002	±	0.0005	0.03	±	0.01	0.002	±	0.0003	0.002	±	0.001	0.03	±	0.005
16:0/22:6	0.03	±	0.002	0.03	±	0.001	0.03	±	0.003	0.02	±	0.003	0.03	±	0.002	0.3	±	0.03	0.03	±	0.002	0.04	±	0.0003	0.3	±	0.03	0.03	±	0.002	0.04	±	0.002	0.3	±	0.02

PC, EVs	DMEM			HEPES			ROL+PA			TGF			DOPC			S80			Ela			DOPC+Ela			S80+Ela			OA			DOPC+OA			S80+OA		
	mean	±	SEM	mean	±	SEM	mean	±	SEM	mean	±	SEM	mean	±	SEM	mean	±	SEM	mean	±	SEM	mean	±	SEM	mean	±	SEM	mean	±	SEM	mean	±	SEM	mean	±	SEM
14:0/16:0	3.7	±	0.9	3.9	±	0.8	2.1	±	0.5	3.9	±	1.0	0.8	±	0.1	0.7	±	0.1	5.9	±	0.1	1.3	±	0.3	1.2	±	0.4	6.0	±	0.2	1.4	±	0.4	1.3	±	0.2
16:0/16:0	42.4	±	12.7	42.8	±	13.0	44.0	±	12.1	46.9	±	13.9	7.2	±	2.6	8.8	±	1.5	20.9	±	1.2	4.1	±	0.6	8.5	±	0.7	19.8	±	0.7	4.4	±	0.9	8.5	±	0.6
16:0/16:1	11.3	±	2.6	10.6	±	2.3	21.8	±	3.8	11.5	±	3.1	2.0	±	0.4	2.4	±	0.4	14.9	±	0.5	2.8	±	0.7	3.4	±	1.0	15.1	±	0.2	3.0	±	1.0	3.3	±	0.7
14:0/18:1	1.5	±	0.4	1.4	±	0.3	0.6	±	0.2	1.4	±	0.4	0.4	±	0.1	0.5	±	0.1	2.0	±	0.1	0.6	±	0.2	0.6	±	0.1	2.1	±	0.1	0.8	±	0.3	0.6	±	0.1
16:0/18:1	16.9	±	3.8	17.2	±	3.8	15.3	±	3.6	15.5	±	3.9	4.4	±	0.5	10.7	±	0.1	23.1	±	0.3	6.4	±	1.3	11.0	±	0.2	23.4	±	0.1	6.8	±	1.6	11.1	±	0.04
16:1/18:1	4.9	±	1.1	4.7	±	1.1	4.1	±	1.0	4.3	±	1.2	1.1	±	0.1	0.4	±	0.1	6.3	±	0.3	1.9	±	0.6	0.7	±	0.2	6.3	±	0.1	2.2	±	0.8	0.7	±	0.1
18:0/18:1	3.7	±	0.7	3.8	±	0.9	2.5	±	0.6	3.3	±	0.8	1.7	±	0.1	10.9	±	0.4	5.6	±	0.1	2.6	±	0.4	10.3	±	0.5	5.7	±	0.2	2.8	±	0.5	10.2	±	0.4
18:1/18:1	11.8	±	2.4	12.0	±	2.9	6.7	±	1.7	9.9	±	2.6	81.2	±	1.83	11.8	±	0.2	16.7	±	0.4	78.3	±	4.3	11.1	±	0.1	16.8	±	0.2	76.6	±	5.7	11.2	±	0.2
14:0/18:2	0.2	±	0.04	0.1	±	0.03	0.1	±	0.01	0.1	±	0.03	0.03	±	0.01	1.1	±	0.1	0.2	±	0.02	0.05	±	0.01	1.1	±	0.2	0.3	±	0.02	0.1	±	0.02	1.0	±	0.2
16:0/18:2	1.8	±	0.4	1.7	±	0.4	1.8	±	0.4	1.6	±	0.4	0.3	±	0.11	21.0	±	0.6	1.8	±	0.02	0.4	±	0.1	20.4	±	1.1	1.9	±	0.1	0.4	±	0.1	20.2	±	0.7
18:0/18:2	0.1	±	0.02	0.1	±	0.03	0.1	±	0.03	0.1	±	0.03	0.02	±	0.01	11.6	±	0.4	0.2	±	0.02	0.01	±	0.003	11.1	±	0.7	0.3	±	0.1	0.01	±	0.004	11.3	±	0.5
18:1/18:2	1.0	±	0.2	1.0	±	0.3	0.5	±	0.1	0.7	±	0.2	0.8	±	0.08	19.7	±	0.8	1.3	±	0.1	1.3	±	0.1	19.9	±	0.7	1.4	±	0.1	1.3	±	0.1	20.1	±	0.5
16:0/20:4	0.2	±	0.04	0.2	±	0.1	0.2	±	0.04	0.2	±	0.1	0.04	±	0.01	0.1	±	0.01	0.3	±	0.01	0.1	±	0.005	0.1	±	0.03	0.3	±	0.004	0.1	±	0.01	0.1	±	0.02
16:1/20:4	0.03	±	0.01	0.04	±	0.01	0.02	±	0.004	0.02	±	0.01	0.01	±	0.002	0.03	±	0.003	0.1	±	0.003	0.01	±	0.002	0.1	±	0.02	0.04	±	0.002	0.01	±	0.003	0.1	±	0.01
18:0/20:4	0.1	±	0.02	0.2	±	0.1	0.1	±	0.03	0.1	±	0.04	0.01	±	0.002	0.04	±	0.01	0.2	±	0.01	0.004	±	0.001	0.1	±	0.01	0.2	±	0.01	0.004	±	0.001	0.1	±	0.01
18:1/20:4	0.1	±	0.02	0.1	±	0.03	0.1	±	0.01	0.1	±	0.02	0.03	±	0.005	0.1	±	0.01	0.1	±	0.01	0.1	±	0.01	0.11	±	0.03	0.1	±	0.01	0.1	±	0.02	0.1	±	0.01
18:1/20:5	0.002	±	0.0005	0.002	±	0.001	0.002	±	0.0003	0.003	±	0.0005	0.001	±	0.0002	0.004	±	0.001	0.006	±	0.001	0.002	±	0.0004	0.008	±	0.002	0.003	±	0.001	0.002	±	0.001	0.007	±	0.001
16:0/22:4	0.1	±	0.02	0.1	±	0.01	0.03	±	0.01	0.1	±	0.01	0.01	±	0.002	0.05	±	0.01	0.1	±	0.003	0.01	±	0.001	0.1	±	0.01	0.1	±	0.004	0.02	±	0.004	0.1	±	0.002
18:0/22:4	0.1	±	0.01	0.1	±	0.02	0.04	±	0.01	0.05	±	0.01	0.01	±	0.002	0.02	±	0.002	0.1	±	0.01	0.02	±	0.004	0.03	±	0.01	0.1	±	0.001	0.02	±	0.01	0.03	±	0.003
18:1/22:4	0.04	±	0.01	0.04	±	0.01	0.02	±	0.003	0.03	±	0.01	0.005	±	0.001	0.02	±	0.003	0.04	±	0.01	0.01	±	0.002	0.02	±	0.01	0.04	±	0.005	0.01	±	0.003	0.02	±	0.002
18:0/22:5	0.02	±	0.004	0.03	±	0.01	0.02	±	0.01	0.03	±	0.01	0.002	±	0.001	0.003	±	0.0004	0.04	±	0.004	0.001	±	0.0002	0.01	±	0.001	0.04	±	0.004	0.001	±	0.0001	0.01	±	0.0002
18:1/22:5	0.01	±	0.003	0.01	±	0.004	0.01	±	0.003	0.01	±	0.005	0.003	±	0.0005	0.01	±	0.001	0.01	±	0.002	0.004	±	0.0001	0.01	±	0.002	0.01	±	0.001	0.005	±	0.001	0.01	±	0.002
18:2/22:5	0.0003	±	0.0002	0.001	±	0.0005	0.0003	±	0.0002	0.0003	±	0.0002	0.0001	±	0.00005	0.003	±	0.0003	0.001	±	0.0001	0.0003	±	0.0001	0.01	±	0.001	0.002	±	0.0002	0.0005	±	0.0001	0.01	±	0.001
16:0/22:6	0.1	±	0.01	0.1	±	0.02	0.1	±	0.01	0.1	±	0.02	0.01	±	0.002	0.02	±	0.001	0.1	±	0.01	0.02	±	0.002	0.02	±	0.01	0.1	±	0.003	0.02	±	0.002	0.03	±	0.005

Figure S7. PC profile of differently treated cells and their EV fractions. Means ± S.E.M. indicate the proportion of individual PC species as percentage of total PC (100%). Heatmaps show fold changes in the proportion of PC species relative to the DMEM control. Data derive from 3 (DMEM, HEPES, ROL+PA, TGF, Ela, DOPC+Ela, S80+Ela, OA, DOPC+OA, S80+OA) or 5 (DOPC, S80) independent experiments. Total lipid concentration for liposomal treatments was 5 mM, Ela or OA concentration 150 nM.

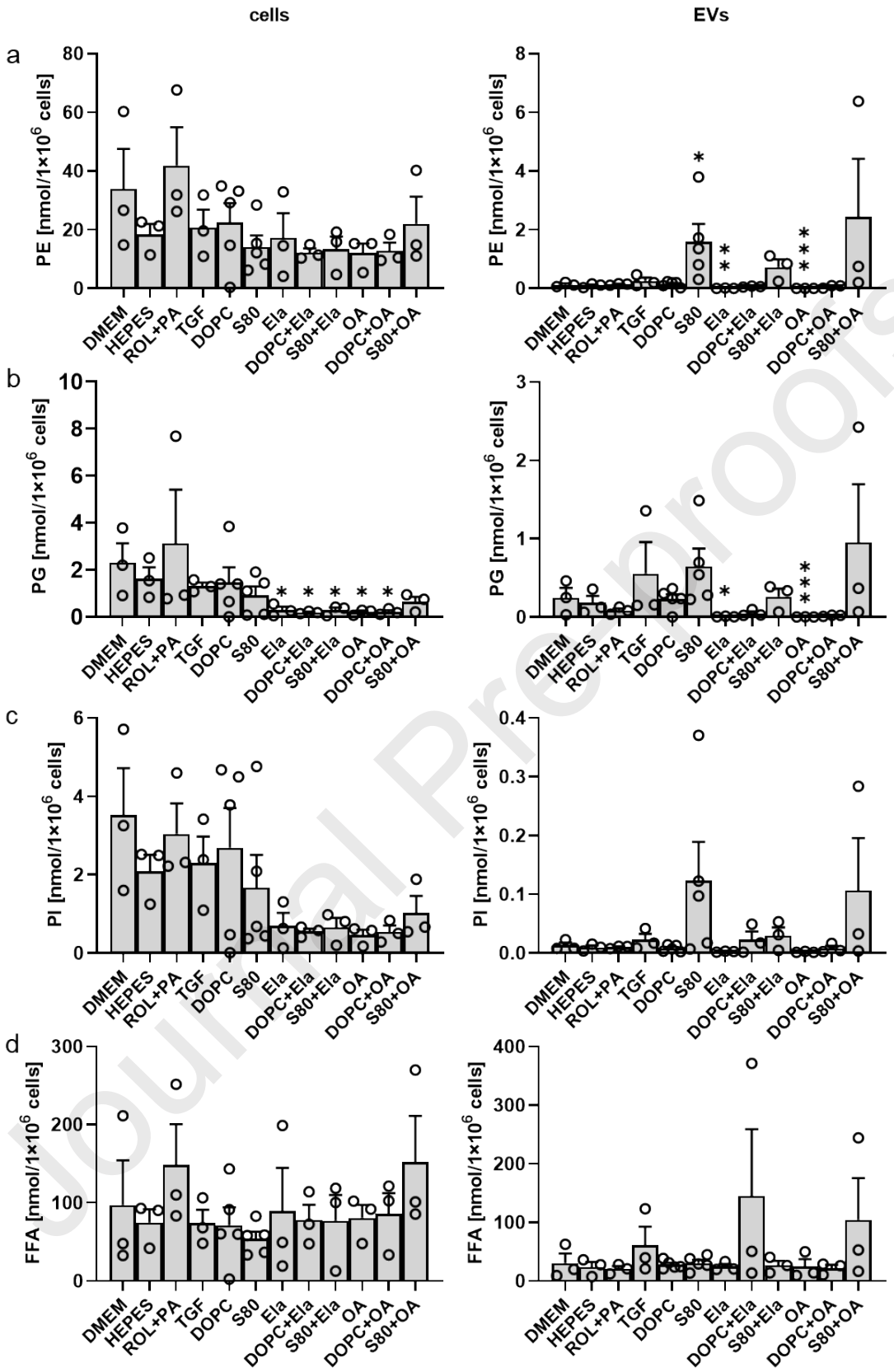

Figure S8. Phospholipid and FFA content of differently treated cells and their EV fractions. Absolute amount of PE (a), PG (b), PI (c), and FFA (d) as sum of the lipid species analyzed within the subclass. Data are presented as means + S.E.M. of 3 (DMEM, HEPES, ROL+PA, TGF, Ela, DOPC+Ela, S80+Ela, OA, DOPC+OA, S80+OA) or 5 (DOPC, S80) independent experiments. Total lipid concentration for liposomal treatments was 5 mM, Ela or OA concentration 150 nM. **P<0.05, **P<0.01, ***P<0.001, mixed-type ANOVA + Dunnett's test of logarithmized values with DMEM as control group.*

0 1 50 fold change

PE, cells	DMEM	HEPES	ROL+PA	TGF	DOPC	S80	Ela	DOPC+Ela	S80+Ela	OA	DOPC+OA	S80+OA
	mean ± SEM	mean ± SEM	mean ± SEM	mean ± SEM	mean ± SEM	mean ± SEM	mean ± SEM	mean ± SEM	mean ± SEM	mean ± SEM	mean ± SEM	mean ± SEM
14:0/16:0	0.6 ± 0.01	0.5 ± 0.01	0.2 ± 0.02	0.5 ± 0.1	0.5 ± 0.02	0.5 ± 0.1	0.5 ± 0.01	0.4 ± 0.01	0.4 ± 0.1	0.5 ± 0.01	0.4 ± 0.04	0.4 ± 0.1
16:0/16:0	1.4 ± 0.1	1.4 ± 0.04	1.1 ± 0.1	1.5 ± 0.04	1.2 ± 0.1	2.3 ± 0.1	1.4 ± 0.1	1.2 ± 0.03	2.0 ± 0.2	1.3 ± 0.03	1.1 ± 0.1	2.0 ± 0.2
16:0/16:1	5.4 ± 0.2	5.0 ± 0.1	15.9 ± 1.2	7.3 ± 0.3	3.9 ± 0.4	2.9 ± 0.4	4.8 ± 0.1	3.4 ± 0.2	2.6 ± 0.2	4.9 ± 0.1	3.0 ± 0.3	2.6 ± 0.2
14:0/18:1	1.1 ± 0.1	1.0 ± 0.04	0.4 ± 0.04	1.1 ± 0.1	1.0 ± 0.04	0.5 ± 0.1	1.0 ± 0.01	1.0 ± 0.02	0.5 ± 0.1	1.1 ± 0.03	0.9 ± 0.1	0.5 ± 0.1
16:0/18:1	10.7 ± 0.1	10.6 ± 0.1	11.3 ± 0.1	10.7 ± 0.2	10.6 ± 0.3	8.5 ± 0.3	10.6 ± 0.2	10.6 ± 0.1	8.5 ± 0.2	10.2 ± 0.3	10.7 ± 0.8	8.5 ± 0.2
16:1/18:1	8.8 ± 0.5	8.5 ± 0.3	11.7 ± 0.5	10.4 ± 0.7	7.1 ± 0.6	2.2 ± 0.3	8.4 ± 0.2	6.6 ± 0.2	2.2 ± 0.2	8.5 ± 0.3	5.8 ± 0.6	2.3 ± 0.2
18:0/18:1	22.5 ± 0.4	23.7 ± 0.4	18.4 ± 1.1	21.0 ± 1.0	25.1 ± 1.2	21.1 ± 1.2	24.5 ± 0.4	24.5 ± 0.4	21.4 ± 0.4	24.8 ± 0.4	24.8 ± 1.5	22.0 ± 0.4
18:1/18:1	37.1 ± 0.9	36.8 ± 0.6	28.6 ± 1.0	35.1 ± 1.2	39.1 ± 1.0	18.1 ± 0.5	37.6 ± 0.1	41.6 ± 0.6	16.4 ± 0.4	37.3 ± 0.6	43.0 ± 1.0	16.6 ± 0.8
16:0/18:2	1.2 ± 0.04	1.1 ± 0.03	2.1 ± 0.2	1.5 ± 0.1	0.9 ± 0.1	3.6 ± 0.2	1.1 ± 0.04	0.8 ± 0.03	4.6 ± 0.7	1.1 ± 0.04	0.7 ± 0.1	4.0 ± 0.5
18:0/18:2	2.5 ± 0.05	2.4 ± 0.05	3.0 ± 0.2	2.5 ± 0.1	2.0 ± 0.2	7.3 ± 0.7	2.0 ± 0.1	1.6 ± 0.1	9.0 ± 1.3	2.1 ± 0.04	1.6 ± 0.05	7.6 ± 1.0
18:1/18:2	1.7 ± 0.1	1.7 ± 0.1	1.5 ± 0.1	1.8 ± 0.1	1.4 ± 0.1	3.4 ± 0.2	1.6 ± 0.04	1.3 ± 0.04	4.4 ± 0.6	1.6 ± 0.1	1.2 ± 0.1	3.8 ± 0.2
16:0/20:3	0.6 ± 0.02	0.5 ± 0.01	0.6 ± 0.04	0.6 ± 0.02	0.5 ± 0.02	0.2 ± 0.01	0.5 ± 0.01	0.6 ± 0.01	0.2 ± 0.02	0.5 ± 0.01	0.5 ± 0.1	0.2 ± 0.02
16:0/20:4	0.5 ± 0.03	0.6 ± 0.03	0.9 ± 0.1	0.6 ± 0.04	0.5 ± 0.04	4.2 ± 0.2	0.5 ± 0.03	0.5 ± 0.001	4.2 ± 0.2	0.5 ± 0.03	0.5 ± 0.1	4.5 ± 0.1
16:1/20:4	0.1 ± 0.004	0.1 ± 0.01	0.1 ± 0.004	0.1 ± 0.01	0.1 ± 0.01	0.2 ± 0.03	0.1 ± 0.003	0.1 ± 0.002	0.2 ± 0.04	0.1 ± 0.004	0.05 ± 0.002	0.2 ± 0.03
18:0/20:4	3.0 ± 0.1	3.2 ± 0.2	2.2 ± 0.1	2.8 ± 0.2	3.2 ± 0.2	11.2 ± 0.8	2.9 ± 0.1	2.9 ± 0.1	11.2 ± 0.4	2.9 ± 0.03	3.0 ± 0.04	11.7 ± 0.1
18:1/20:4	1.1 ± 0.05	1.1 ± 0.1	0.6 ± 0.05	0.9 ± 0.1	1.2 ± 0.1	4.3 ± 0.3	1.0 ± 0.03	1.3 ± 0.03	4.3 ± 0.4	1.1 ± 0.1	1.2 ± 0.1	4.4 ± 0.4
16:0/22:4	0.1 ± 0.0005	0.1 ± 0.002	0.1 ± 0.003	0.1 ± 0.001	0.1 ± 0.03	0.05 ± 0.002	0.1 ± 0.001	0.1 ± 0.01	0.04 ± 0.001	0.1 ± 0.0005	0.2 ± 0.01	0.04 ± 0.002
16:1/22:4	0.01 ± 0.0004	0.01 ± 0.0005	0.01 ± 0.0002	0.01 ± 0.001	0.01 ± 0.001	0.01 ± 0.001	0.01 ± 0.001	0.01 ± 0.001	0.01 ± 0.0004	0.01 ± 0.0004	0.01 ± 0.002	0.01 ± 0.001
18:0/22:4	0.7 ± 0.02	0.7 ± 0.03	0.5 ± 0.01	0.6 ± 0.03	0.6 ± 0.03	3.4 ± 0.2	0.6 ± 0.02	0.5 ± 0.02	3.0 ± 0.1	0.6 ± 0.01	0.5 ± 0.01	3.2 ± 0.2
18:1/22:4	0.4 ± 0.01	0.3 ± 0.01	0.2 ± 0.01	0.3 ± 0.02	0.3 ± 0.02	1.6 ± 0.1	0.3 ± 0.01	0.3 ± 0.002	1.3 ± 0.04	0.3 ± 0.01	0.3 ± 0.01	1.3 ± 0.02
16:0/22:5	0.04 ± 0.001	0.04 ± 0.002	0.04 ± 0.01	0.04 ± 0.003	0.04 ± 0.001	0.6 ± 0.05	0.04 ± 0.002	0.05 ± 0.003	0.5 ± 0.1	0.04 ± 0.002	0.04 ± 0.002	0.6 ± 0.1
18:0/22:5	0.3 ± 0.01	0.4 ± 0.01	0.3 ± 0.02	0.3 ± 0.02	0.4 ± 0.02	2.1 ± 0.1	0.3 ± 0.002	0.3 ± 0.01	1.7 ± 0.3	0.3 ± 0.01	0.3 ± 0.01	1.9 ± 0.1
18:1/22:5	0.1 ± 0.003	0.1 ± 0.003	0.05 ± 0.003	0.1 ± 0.004	0.1 ± 0.01	0.6 ± 0.04	0.1 ± 0.002	0.1 ± 0.004	0.5 ± 0.1	0.1 ± 0.003	0.1 ± 0.01	0.6 ± 0.1
16:0/22:6	0.1 ± 0.01	0.1 ± 0.01	0.2 ± 0.02	0.1 ± 0.02	0.1 ± 0.01	1.0 ± 0.1	0.1 ± 0.01	0.1 ± 0.01	0.9 ± 0.1	0.1 ± 0.01	0.1 ± 0.02	1.0 ± 0.1

PE, EVs	DMEM	HEPES	ROL+PA	TGF	DOPC	S80	Ela	DOPC+Ela	S80+Ela	OA	DOPC+OA	S80+OA
	mean ± SEM	mean ± SEM	mean ± SEM	mean ± SEM	mean ± SEM	mean ± SEM	mean ± SEM	mean ± SEM	mean ± SEM	mean ± SEM	mean ± SEM	mean ± SEM
14:0/16:0	0.4 ± 0.02	0.3 ± 0.02	0.1 ± 0.01	0.2 ± 0.02	0.2 ± 0.03	0.2 ± 0.05	1.9 ± 0.8	0.5 ± 0.2	0.2 ± 0.04	1.7 ± 0.5	0.4 ± 0.2	0.2 ± 0.02
16:0/16:0	1.5 ± 0.4	1.6 ± 0.6	0.8 ± 0.2	1.1 ± 0.3	0.7 ± 0.2	1.3 ± 0.3	2.6 ± 0.8	1.0 ± 0.3	1.2 ± 0.2	2.3 ± 0.4	0.8 ± 0.2	1.2 ± 0.2
16:0/16:1	3.1 ± 0.3	2.6 ± 0.2	9.6 ± 1.0	2.9 ± 0.1	1.3 ± 0.1	1.1 ± 0.2	3.3 ± 0.3	1.1 ± 0.1	1.1 ± 0.2	3.4 ± 0.5	1.1 ± 0.03	1.1 ± 0.1
14:0/18:1	0.6 ± 0.1	0.5 ± 0.03	0.2 ± 0.01	0.5 ± 0.01	0.3 ± 0.02	0.2 ± 0.05	0.7 ± 0.1	0.3 ± 0.05	0.2 ± 0.04	0.9 ± 0.0	0.3 ± 0.04	0.2 ± 0.02
16:0/18:1	11.2 ± 0.9	9.5 ± 0.3	12.5 ± 0.2	9.4 ± 0.2	5.9 ± 0.2	9.5 ± 0.7	11.4 ± 0.9	5.6 ± 0.5	9.2 ± 0.8	11.7 ± 0.5	5.9 ± 0.5	9.1 ± 0.6
16:1/18:1	3.9 ± 0.6	3.2 ± 0.1	4.7 ± 0.2	3.3 ± 0.05	1.8 ± 0.2	0.9 ± 0.1	3.6 ± 0.3	1.3 ± 0.3	1.2 ± 0.1	4.4 ± 0.2	1.4 ± 0.2	1.2 ± 0.02
18:0/18:1	33.1 ± 2.0	37.6 ± 0.8	34.4 ± 1.4	37.1 ± 0.6	21.3 ± 0.7	8.7 ± 0.8	38.0 ± 1.0	17.2 ± 2.6	11.2 ± 1.1	38.5 ± 1.1	18.4 ± 0.8	11.5 ± 0.4
18:1/18:1	37.8 ± 1.0	36.5 ± 0.7	28.5 ± 0.7	37.3 ± 1.0	59.6 ± 1.7	12.3 ± 1.5	31.5 ± 2.6	63.7 ± 1.8	11.9 ± 0.7	29.6 ± 1.4	63.3 ± 0.4	11.7 ± 0.3
16:0/18:2	0.6 ± 0.1	0.6 ± 0.03	1.0 ± 0.1	0.6 ± 0.01	0.3 ± 0.1	31.9 ± 3.9	0.8 ± 0.1	0.8 ± 0.4	32.4 ± 1.8	0.7 ± 0.1	0.6 ± 0.3	34.9 ± 1.0
18:0/18:2	1.9 ± 0.04	1.9 ± 0.01	2.5 ± 0.1	2.1 ± 0.02	1.8 ± 0.1	10.6 ± 0.4	1.6 ± 0.5	2.7 ± 0.9	10.2 ± 0.8	1.3 ± 0.2	2.2 ± 0.7	8.6 ± 0.4
18:1/18:2	0.8 ± 0.1	0.7 ± 0.02	0.7 ± 0.01	0.7 ± 0.04	0.4 ± 0.1	17.7 ± 0.8	0.5 ± 0.1	1.0 ± 0.3	15.3 ± 1.1	1.0 ± 0.4	0.9 ± 0.3	14.3 ± 0.7
16:0/20:3	0.4 ± 0.1	0.3 ± 0.02	0.5 ± 0.03	0.3 ± 0.02	0.2 ± 0.01	0.1 ± 0.01	0.3 ± 0.1	0.1 ± 0.04	0.1 ± 0.02	0.4 ± 0.1	0.2 ± 0.01	0.1 ± 0.02
16:0/20:4	0.3 ± 0.04	0.3 ± 0.01	0.5 ± 0.02	0.3 ± 0.02	0.2 ± 0.02	0.7 ± 0.1	0.2 ± 0.1	0.1 ± 0.02	0.9 ± 0.2	0.3 ± 0.03	0.1 ± 0.03	0.9 ± 0.2
16:1/20:4	0.03 ± 0.01	0.03 ± 0.002	0.03 ± 0.002	0.03 ± 0.002	0.02 ± 0.003	0.02 ± 0.003	0.1 ± 0.04	0.01 ± 0.01	0.02 ± 0.01	0.1 ± 0.03	0.01 ± 0.004	0.03 ± 0.01
18:0/20:4	2.5 ± 0.2	2.6 ± 0.1	2.2 ± 0.04	2.3 ± 0.2	4.6 ± 0.4	2.6 ± 0.2	1.6 ± 0.5	3.1 ± 0.6	2.7 ± 0.6	2.2 ± 0.1	3.1 ± 0.6	2.7 ± 0.6
18:1/20:4	0.6 ± 0.1	0.5 ± 0.02	0.3 ± 0.005	0.4 ± 0.01	0.4 ± 0.03	1.1 ± 0.1	0.6 ± 0.1	0.3 ± 0.1	1.2 ± 0.3	0.4 ± 0.1	0.3 ± 0.04	1.2 ± 0.3
16:0/22:4	0.1 ± 0.01	0.1 ± 0.01	0.1 ± 0.004	0.1 ± 0.001	0.1 ± 0.01	0.01 ± 0.001	0.02 ± 0.01	0.1 ± 0.02	0.02 ± 0.003	0.05 ± 0.01	0.1 ± 0.01	0.02 ± 0.01
16:1/22:4	0.01 ± 0.001	0.005 ± 0.0003	0.003 ± 0.0004	0.01 ± 0.001	0.01 ± 0.003	0.01 ± 0.002	0.1 ± 0.03	0.01 ± 0.01	0.01 ± 0.001	0.04 ± 0.01	0.01 ± 0.004	0.01 ± 0.001
18:0/22:4	0.6 ± 0.02	0.6 ± 0.02	0.6 ± 0.01	0.7 ± 0.01	0.3 ± 0.03	0.4 ± 0.05	0.7 ± 0.1	0.4 ± 0.03	0.5 ± 0.1	0.3 ± 0.1	0.3 ± 0.03	0.5 ± 0.1
18:1/22:4	0.2 ± 0.01	0.2 ± 0.005	0.1 ± 0.002	0.2 ± 0.003	0.3 ± 0.02	0.3 ± 0.03	0.2 ± 0.04	0.4 ± 0.1	0.2 ± 0.1	0.3 ± 0.1	0.3 ± 0.1	0.2 ± 0.1
16:0/22:5	0.04 ± 0.005	0.04 ± 0.005	0.05 ± 0.01	0.04 ± 0.01	0.02 ± 0.003	0.1 ± 0.01	0.1 ± 0.04	0.03 ± 0.01	0.1 ± 0.03	0.1 ± 0.01	0.01 ± 0.003	0.1 ± 0.03
18:0/22:5	0.3 ± 0.01	0.3 ± 0.01	0.3 ± 0.004	0.3 ± 0.003	0.2 ± 0.01	0.2 ± 0.01	0.2 ± 0.1	0.1 ± 0.01	0.2 ± 0.1	0.2 ± 0.1	0.1 ± 0.02	0.2 ± 0.1
18:1/22:5	0.1 ± 0.005	0.1 ± 0.001	0.03 ± 0.001	0.04 ± 0.003	0.04 ± 0.004	0.1 ± 0.005	0.03 ± 0.004	0.05 ± 0.01	0.1 ± 0.03	0.1 ± 0.04	0.1 ± 0.03	0.1 ± 0.03
16:0/22:6	0.1 ± 0.02	0.1 ± 0.004	0.1 ± 0.004	0.1 ± 0.004	0.04 ± 0.01	0.1 ± 0.01	0.04 ± 0.02	0.03 ± 0.01	0.1 ± 0.03	0.1 ± 0.03	0.04 ± 0.02	0.1 ± 0.03

Figure S9. PE profile of differently treated cells and their EV fractions. Means ± S.E.M. indicate the proportion of individual PE species as percentage of total PE (100%). Heatmaps show fold changes in the proportion of PE species relative to the DMEM control. Data derive from 3 (DMEM, HEPES, ROL+PA, TGF, Ela, DOPC+Ela, S80+Ela, OA, DOPC+OA, S80+OA) or 5 (DOPC, S80) independent experiments. Total lipid concentration for liposomal treatments was 5 mM, Ela or OA concentration 150 nM.

0 1 30 fold change

PI, cells	DMEM	HEPES	ROL+PA	TGF	DOPC	S80	Ela	DOPC+Ela	S80+Ela	OA	DOPC+OA	S80+OA
	mean ± SEM	mean ± SEM	mean ± SEM	mean ± SEM	mean ± SEM	mean ± SEM	mean ± SEM	mean ± SEM	mean ± SEM	mean ± SEM	mean ± SEM	mean ± SEM
14:0/16:0	0.01 ± 0.002	0.01 ± 0.001	0.01 ± 0.002	0.1 ± 0.01	0.01 ± 0.0004	0.01 ± 0.002						
16:0/16:0	0.2 ± 0.01	0.2 ± 0.004	1.0 ± 0.1	0.9 ± 0.1	0.2 ± 0.01	0.3 ± 0.05	0.2 ± 0.05	0.2 ± 0.02	0.3 ± 0.03	0.2 ± 0.03	0.1 ± 0.05	0.4 ± 0.01
16:0/16:1	1.3 ± 0.1	1.1 ± 0.1	3.5 ± 0.5	2.9 ± 0.2	1.0 ± 0.1	0.6 ± 0.03	1.3 ± 0.1	0.9 ± 0.03	0.5 ± 0.1	1.4 ± 0.1	0.9 ± 0.1	0.6 ± 0.03
14:0/18:1	0.2 ± 0.02	0.2 ± 0.01	0.1 ± 0.003	0.6 ± 0.1	0.1 ± 0.01	0.1 ± 0.01	0.2 ± 0.02	0.1 ± 0.01	0.1 ± 0.02	0.2 ± 0.01	0.1 ± 0.02	0.1 ± 0.01
16:0/18:1	3.1 ± 0.1	3.0 ± 0.1	5.5 ± 0.2	6.2 ± 0.3	2.7 ± 0.1	1.8 ± 0.2	2.9 ± 0.2	2.5 ± 0.03	1.6 ± 0.1	2.8 ± 0.1	2.7 ± 0.2	1.8 ± 0.1
16:1/18:1	6.7 ± 0.2	6.4 ± 0.1	6.9 ± 0.2	10.9 ± 0.1	5.4 ± 0.4	1.7 ± 0.1	7.3 ± 0.1	4.6 ± 0.03	1.5 ± 0.3	6.8 ± 0.3	5.0 ± 0.4	1.7 ± 0.2
18:0/18:1	9.8 ± 0.6	8.9 ± 0.4	12.8 ± 0.2	11.0 ± 0.7	7.6 ± 0.8	4.8 ± 0.8	6.4 ± 0.1	5.8 ± 0.02	3.3 ± 0.05	6.2 ± 0.1	6.0 ± 0.1	3.6 ± 0.1
18:1/18:1	18.0 ± 0.9	19.3 ± 1.3	10.7 ± 1.5	19.2 ± 1.1	17.0 ± 0.8	6.1 ± 0.8	15.7 ± 0.2	16.5 ± 0.3	4.2 ± 0.5	15.2 ± 0.6	16.0 ± 0.3	4.7 ± 0.5
16:0/18:2	0.9 ± 0.02	0.8 ± 0.04	2.0 ± 0.2	1.9 ± 0.1	0.9 ± 0.2	1.5 ± 0.1	1.6 ± 0.02	1.0 ± 0.02	1.6 ± 0.1	1.6 ± 0.01	1.1 ± 0.1	1.5 ± 0.03
18:0/18:2	2.5 ± 0.2	2.3 ± 0.2	6.4 ± 0.6	3.3 ± 0.2	1.7 ± 0.2	11.7 ± 1.3	2.7 ± 0.3	1.5 ± 0.1	11.0 ± 1.5	2.5 ± 0.1	1.4 ± 0.1	9.2 ± 0.7
18:1/18:2	2.5 ± 0.2	2.7 ± 0.2	1.7 ± 0.2	3.3 ± 0.2	1.9 ± 0.2	2.7 ± 0.4	2.1 ± 0.2	1.3 ± 0.03	2.4 ± 0.3	2.0 ± 0.1	1.3 ± 0.1	2.3 ± 0.1
16:0/20:3	2.0 ± 0.01	2.0 ± 0.1	3.3 ± 0.3	2.3 ± 0.1	2.8 ± 0.5	0.4 ± 0.04	3.4 ± 0.1	3.2 ± 0.1	0.4 ± 0.1	3.3 ± 0.1	3.5 ± 0.1	0.5 ± 0.1
18:0/20:3	40.0 ± 1.4	38.9 ± 1.4	36.8 ± 1.2	26.4 ± 0.4	43.8 ± 1.1	6.1 ± 0.5	39.8 ± 0.4	45.7 ± 0.5	5.7 ± 0.6	41.3 ± 0.7	45.0 ± 0.8	6.0 ± 0.9
18:1/20:3	8.0 ± 0.5	9.1 ± 0.6	3.1 ± 0.5	6.9 ± 0.5	9.4 ± 0.4	0.7 ± 0.1	9.6 ± 0.1	10.8 ± 0.2	0.6 ± 0.1	9.5 ± 0.2	10.5 ± 0.4	0.6 ± 0.2
16:0/20:4	0.3 ± 0.003	0.3 ± 0.01	0.6 ± 0.1	0.3 ± 0.01	0.4 ± 0.1	4.5 ± 0.7	0.5 ± 0.02	0.4 ± 0.02	4.7 ± 0.5	0.5 ± 0.02	0.4 ± 0.1	5.1 ± 0.3
16:1/20:4	0.03 ± 0.003	0.03 ± 0.003	0.03 ± 0.01	0.03 ± 0.003	0.04 ± 0.01	0.2 ± 0.04	0.04 ± 0.01	0.04 ± 0.01	0.2 ± 0.04	0.04 ± 0.003	0.04 ± 0.002	0.2 ± 0.03
18:0/20:4	3.6 ± 0.2	3.7 ± 0.1	4.9 ± 0.2	2.9 ± 0.2	3.9 ± 0.3	49.2 ± 2.2	5.1 ± 0.1	4.4 ± 0.05	54.8 ± 0.9	5.1 ± 0.2	4.6 ± 0.3	54.1 ± 1.6
18:1/20:4	0.9 ± 0.1	1.1 ± 0.1	0.6 ± 0.1	1.0 ± 0.1	1.1 ± 0.1	7.5 ± 0.6	1.4 ± 0.1	1.1 ± 0.04	7.1 ± 0.4	1.4 ± 0.02	1.2 ± 0.1	7.7 ± 0.3

PI, EVs	DMEM	HEPES	ROL+PA	TGF	DOPC	S80	Ela	DOPC+Ela	S80+Ela	OA	DOPC+OA	S80+OA
	mean ± SEM	mean ± SEM	mean ± SEM	mean ± SEM	mean ± SEM	mean ± SEM	mean ± SEM	mean ± SEM	mean ± SEM	mean ± SEM	mean ± SEM	mean ± SEM
14:0/16:0	0.1 ± 0.01	0.1 ± 0.01	0.05 ± 0.02	0.1 ± 0.01	0.04 ± 0.005	0.02 ± 0.002						
16:0/16:0	0.8 ± 0.04	0.8 ± 0.1	4.1 ± 0.4	1.5 ± 0.2	0.6 ± 0.1	0.8 ± 0.04	1.0 ± 0.4	0.7 ± 0.01	1.0 ± 0.2	0.6 ± 0.2	0.7 ± 0.1	1.1 ± 0.1
16:0/16:1	2.1 ± 0.1	1.9 ± 0.2	5.4 ± 0.4	3.0 ± 0.1	1.6 ± 0.2	0.4 ± 0.03	2.1 ± 0.2	1.4 ± 0.1	0.7 ± 0.1	2.3 ± 0.2	1.4 ± 0.1	0.7 ± 0.04
14:0/18:1	0.3 ± 0.02	0.3 ± 0.03	0.2 ± 0.02	0.4 ± 0.03	0.3 ± 0.03	0.1 ± 0.01	0.6 ± 0.2	0.3 ± 0.1	0.1 ± 0.02	0.7 ± 0.2	0.4 ± 0.1	0.2 ± 0.03
16:0/18:1	6.1 ± 0.1	6.0 ± 0.1	9.0 ± 0.2	7.8 ± 0.4	5.0 ± 0.2	4.6 ± 0.3	5.3 ± 0.2	5.2 ± 0.2	4.0 ± 0.1	5.6 ± 0.2	4.8 ± 0.4	4.0 ± 0.1
16:1/18:1	5.6 ± 0.2	5.6 ± 0.1	5.4 ± 0.1	6.7 ± 0.1	4.8 ± 0.3	1.0 ± 0.1	6.9 ± 0.8	4.8 ± 0.3	1.3 ± 0.2	6.4 ± 0.2	4.4 ± 0.2	1.4 ± 0.03
18:0/18:1	15.2 ± 0.6	14.9 ± 0.3	16.7 ± 0.7	16.1 ± 0.5	12.6 ± 1.0	3.9 ± 0.5	9.7 ± 0.1	11.3 ± 1.4	3.4 ± 0.3	10.6 ± 0.6	12.1 ± 0.9	3.8 ± 0.2
18:1/18:1	16.6 ± 0.3	17.8 ± 0.7	8.5 ± 1.0	17.1 ± 0.6	20.0 ± 1.4	3.6 ± 0.6	16.7 ± 0.6	20.1 ± 2.3	3.8 ± 0.4	15.4 ± 0.2	21.8 ± 2.2	4.2 ± 0.2
16:0/18:2	1.2 ± 0.1	1.3 ± 0.04	2.7 ± 0.2	1.7 ± 0.1	1.3 ± 0.3	46.0 ± 4.5	2.1 ± 0.1	1.3 ± 0.1	36.9 ± 4.6	2.3 ± 0.2	1.2 ± 0.1	33.4 ± 1.1
18:0/18:2	2.8 ± 0.2	2.6 ± 0.1	5.6 ± 0.3	2.9 ± 0.2	1.9 ± 0.2	13.0 ± 1.6	2.9 ± 0.4	1.7 ± 0.2	11.9 ± 1.3	3.0 ± 0.3	1.4 ± 0.1	12.4 ± 1.4
18:1/18:2	1.9 ± 0.03	2.1 ± 0.1	1.4 ± 0.1	2.3 ± 0.2	1.4 ± 0.2	5.3 ± 0.2	1.6 ± 0.1	1.1 ± 0.2	5.8 ± 0.4	1.6 ± 0.1	1.3 ± 0.1	6.0 ± 0.7
16:0/20:3	2.8 ± 0.02	2.5 ± 0.1	3.4 ± 0.1	2.7 ± 0.2	3.0 ± 0.3	0.3 ± 0.03	3.7 ± 0.2	2.9 ± 0.5	0.5 ± 0.1	3.8 ± 0.3	2.7 ± 0.3	0.5 ± 0.1
18:0/20:3	31.1 ± 0.3	30.0 ± 0.5	27.1 ± 0.7	25.5 ± 0.6	32.3 ± 0.7	3.6 ± 0.4	28.9 ± 0.4	33.5 ± 1.2	5.2 ± 0.9	30.0 ± 1.0	32.6 ± 0.5	5.3 ± 0.6
18:1/20:3	5.8 ± 0.2	6.4 ± 0.3	2.5 ± 0.2	5.1 ± 0.2	7.5 ± 0.4	0.4 ± 0.05	7.5 ± 0.4	7.2 ± 0.2	0.7 ± 0.2	6.8 ± 0.4	7.2 ± 0.6	0.7 ± 0.1
16:0/20:4	0.8 ± 0.1	0.7 ± 0.03	1.2 ± 0.04	0.7 ± 0.04	0.6 ± 0.1	1.8 ± 0.3	0.9 ± 0.1	0.7 ± 0.1	2.7 ± 0.9	1.4 ± 0.2	0.6 ± 0.1	2.6 ± 0.7
16:1/20:4	0.1 ± 0.01	0.04 ± 0.01	0.01 ± 0.01	0.1 ± 0.004	0.04 ± 0.01	0.1 ± 0.005	0.1 ± 0.1	0.04 ± 0.004	0.1 ± 0.05	0.1 ± 0.01	0.03 ± 0.02	0.1 ± 0.02
18:0/20:4	5.3 ± 0.1	5.6 ± 0.04	6.0 ± 0.1	5.2 ± 0.1	5.6 ± 0.4	12.8 ± 1.7	7.6 ± 0.3	5.9 ± 1.1	18.4 ± 2.2	7.4 ± 0.4	5.8 ± 0.9	19.7 ± 1.0
18:1/20:4	1.4 ± 0.1	1.5 ± 0.1	0.8 ± 0.1	1.3 ± 0.1	1.6 ± 0.2	2.3 ± 0.3	2.2 ± 0.3	1.8 ± 0.3	3.6 ± 0.8	2.0 ± 0.1	1.6 ± 0.3	3.8 ± 0.4

Figure S10. PI profile of differently treated cells and their EV fractions. Means ± S.E.M. indicate the proportion of individual PI species as percentage of total PI (100%). Heatmaps show fold changes in the proportion of PI species relative to the DMEM control. Data derive from 3 (DMEM, HEPES, ROL+PA, TGF, Ela, DOPC+Ela, S80+Ela, OA, DOPC+OA, S80+OA) or 5 (DOPC, S80) independent experiments. Total lipid concentration for liposomal treatments was 5 mM, Ela or OA concentration 150 nM.

0 1 250 fold change

PG, cells	DMEM	HEPES	ROL+PA	TGF	DOPC	S80	Ela	DOPC+Ela	S80+Ela	OA	DOPC+OA	S80+OA
	mean ± SEM	mean ± SEM	mean ± SEM	mean ± SEM	mean ± SEM	mean ± SEM	mean ± SEM	mean ± SEM	mean ± SEM	mean ± SEM	mean ± SEM	mean ± SEM
14:0/16:0	0.2 ± 0.1	0.2 ± 0.1	0.1 ± 0.04	0.2 ± 0.05	0.3 ± 0.1	0.5 ± 0.2	0.7 ± 0.1	0.7 ± 0.1	0.5 ± 0.1	0.7 ± 0.1	0.7 ± 0.1	0.4 ± 0.1
16:0/16:0	0.9 ± 0.4	0.8 ± 0.3	1.7 ± 0.6	1.0 ± 0.2	1.5 ± 0.5	3.4 ± 1.3	2.9 ± 0.2	3.3 ± 0.1	5.4 ± 1.4	2.8 ± 0.1	3.1 ± 0.3	4.1 ± 1.3
18:0/18:0	0.3 ± 0.1	0.2 ± 0.1	0.9 ± 0.9	1.0 ± 0.8	0.3 ± 0.2	0.3 ± 0.1	0.8 ± 0.3	0.9 ± 0.3	1.6 ± 0.5	0.7 ± 0.3	1.7 ± 1.2	1.0 ± 0.4
16:0/16:1	1.0 ± 0.4	0.8 ± 0.3	1.7 ± 0.5	1.1 ± 0.2	1.5 ± 0.6	1.3 ± 0.5	3.8 ± 0.1	3.2 ± 0.1	1.7 ± 0.4	3.5 ± 0.3	3.0 ± 0.4	1.3 ± 0.4
14:0/18:1	0.2 ± 0.1	0.2 ± 0.1	0.1 ± 0.04	0.2 ± 0.05	0.4 ± 0.1	0.5 ± 0.2	0.9 ± 0.02	0.9 ± 0.03	0.6 ± 0.2	0.9 ± 0.1	0.9 ± 0.1	0.4 ± 0.2
16:0/18:1	4.8 ± 2.0	3.9 ± 1.7	7.8 ± 2.5	4.5 ± 0.7	6.9 ± 2.1	12.1 ± 4.1	16.0 ± 0.3	17.5 ± 0.9	17.8 ± 1.6	15.2 ± 0.4	15.8 ± 1.4	15.2 ± 5.4
16:1/18:1	1.6 ± 0.6	1.4 ± 0.6	2.0 ± 0.6	1.5 ± 0.3	2.5 ± 0.8	1.9 ± 0.7	5.4 ± 0.3	4.9 ± 0.1	2.3 ± 0.3	5.0 ± 0.2	4.4 ± 0.3	2.0 ± 0.7
18:0/18:1	10.4 ± 4.5	8.1 ± 3.6	15.7 ± 5.9	9.1 ± 2.3	17.8 ± 6.8	18.8 ± 6.9	44.8 ± 1.6	45.6 ± 1.5	27.2 ± 4.2	47.3 ± 1.6	46.9 ± 4.2	22.4 ± 7.8
18:1/18:1	76.2 ± 9.9	81.5 ± 7.8	64.0 ± 12.5	76.9 ± 5.0	63.6 ± 13.0	49.2 ± 18.6	12.7 ± 0.8	13.0 ± 0.5	25.9 ± 8.0	11.7 ± 0.1	12.9 ± 0.8	39.0 ± 21.5
16:0/18:2	0.2 ± 0.1	0.2 ± 0.1	0.3 ± 0.1	0.2 ± 0.05	0.3 ± 0.1	1.8 ± 0.7	0.6 ± 0.02	0.5 ± 0.04	2.8 ± 0.1	0.6 ± 0.1	0.5 ± 0.04	2.1 ± 0.8
18:0/18:2	0.9 ± 0.4	0.6 ± 0.3	0.8 ± 0.3	0.6 ± 0.1	1.1 ± 0.4	4.0 ± 1.6	2.9 ± 0.1	2.4 ± 0.1	6.0 ± 0.2	2.9 ± 0.2	2.5 ± 0.1	5.1 ± 1.9
18:1/18:2	3.2 ± 1.3	2.2 ± 0.9	4.7 ± 1.5	3.6 ± 0.7	3.6 ± 1.2	3.1 ± 1.1	8.3 ± 0.5	6.8 ± 0.5	4.6 ± 0.4	8.4 ± 0.5	7.1 ± 1.5	3.8 ± 1.5
16:0/20:4	0.03 ± 0.01	0.03 ± 0.01	0.1 ± 0.02	0.02 ± 0.01	0.1 ± 0.04	1.8 ± 0.8	0.1 ± 0.01	0.1 ± 0.004	2.1 ± 0.4	0.1 ± 0.03	0.1 ± 0.02	1.6 ± 0.5
18:0/20:4	0.04 ± 0.02	0.03 ± 0.01	0.1 ± 0.02	0.03 ± 0.01	0.1 ± 0.03	1.4 ± 0.6	0.2 ± 0.01	0.2 ± 0.01	1.6 ± 0.1	0.2 ± 0.04	0.2 ± 0.03	1.4 ± 0.5

PG, EVs	DMEM	HEPES	ROL+PA	TGF	DOPC	S80	Ela	DOPC+Ela	S80+Ela	OA	DOPC+OA	S80+OA
	mean ± SEM	mean ± SEM	mean ± SEM	mean ± SEM	mean ± SEM	mean ± SEM	mean ± SEM	mean ± SEM	mean ± SEM	mean ± SEM	mean ± SEM	mean ± SEM
14:0/16:0	0.04 ± 0.03	0.02 ± 0.005	0.04 ± 0.01	0.03 ± 0.01	0.3 ± 0.3	0.2 ± 0.04	1.8 ± 0.8	0.6 ± 0.3	0.3 ± 0.03	2.6 ± 0.4	0.7 ± 0.3	0.2 ± 0.03
16:0/16:0	0.1 ± 0.1	0.1 ± 0.002	0.2 ± 0.1	0.1 ± 0.02	0.8 ± 0.7	5.2 ± 1.0	2.3 ± 1.0	1.2 ± 0.5	6.6 ± 0.7	3.4 ± 0.5	1.3 ± 0.7	5.4 ± 0.9
18:0/18:0	1.0 ± 0.7	0.2 ± 0.1	1.3 ± 1.1	0.1 ± 0.02	3.8 ± 3.5	0.5 ± 0.2	8.3 ± 6.1	32.2 ± 18.3	1.7 ± 0.2	11.0 ± 2.2	30.4 ± 17.6	2.5 ± 0.7
16:0/16:1	0.1 ± 0.1	0.05 ± 0.01	0.3 ± 0.1	0.1 ± 0.03	0.6 ± 0.6	0.2 ± 0.04	2.6 ± 1.1	1.0 ± 0.5	0.3 ± 0.03	3.8 ± 0.1	1.0 ± 0.5	0.3 ± 0.05
14:0/18:1	0.04 ± 0.02	0.02 ± 0.002	0.03 ± 0.01	0.02 ± 0.01	0.3 ± 0.3	0.1 ± 0.01	1.1 ± 0.5	0.6 ± 0.3	0.1 ± 0.004	1.2 ± 0.1	0.5 ± 0.2	0.1 ± 0.01
16:0/18:1	0.5 ± 0.3	0.2 ± 0.01	0.8 ± 0.2	0.3 ± 0.1	3.2 ± 3.0	8.2 ± 1.7	11.0 ± 4.5	6.6 ± 3.3	10.2 ± 1.0	16.3 ± 0.3	7.0 ± 3.2	8.4 ± 1.1
16:1/18:1	0.3 ± 0.2	0.2 ± 0.02	0.4 ± 0.1	0.2 ± 0.1	2.2 ± 2.1	0.1 ± 0.02	8.1 ± 3.3	4.0 ± 2.0	0.3 ± 0.1	11.4 ± 0.3	4.1 ± 1.9	0.3 ± 0.1
18:0/18:1	0.5 ± 0.3	0.3 ± 0.03	0.8 ± 0.2	0.3 ± 0.1	3.4 ± 3.3	1.2 ± 0.2	12.8 ± 5.3	8.9 ± 4.9	3.6 ± 1.0	18.0 ± 0.9	10.1 ± 5.3	3.3 ± 0.9
18:1/18:1	97.3 ± 1.0	98.9 ± 0.1	96.0 ± 1.7	98.8 ± 0.4	84.3 ± 14.7	33.8 ± 9.6	47.2 ± 21.4	42.3 ± 26.6	3.0 ± 0.2	25.6 ± 2.2	42.0 ± 25.5	10.3 ± 7.7
16:0/18:2	0.03 ± 0.02	0.01 ± 0.001	0.04 ± 0.01	0.02 ± 0.004	0.2 ± 0.1	40.6 ± 6.9	0.7 ± 0.3	0.5 ± 0.2	60.7 ± 3.9	1.3 ± 0.2	0.6 ± 0.2	57.8 ± 3.9
18:0/18:2	0.04 ± 0.03	0.02 ± 0.002	0.1 ± 0.02	0.03 ± 0.01	0.3 ± 0.2	4.8 ± 0.8	1.6 ± 0.8	1.1 ± 0.5	6.2 ± 0.8	2.2 ± 0.5	1.2 ± 0.5	5.4 ± 0.8
18:1/18:2	0.1 ± 0.1	0.1 ± 0.001	0.2 ± 0.04	0.1 ± 0.03	0.6 ± 0.5	5.0 ± 1.0	2.0 ± 0.9	1.0 ± 0.4	6.8 ± 0.7	2.9 ± 0.2	0.9 ± 0.4	5.9 ± 1.1
16:0/20:4	0.003 ± 0.002	0.002 ± 0.0002	0.01 ± 0.002	0.001 ± 0.001	0.04 ± 0.04	0.05 ± 0.01	0.1 ± 0.03	0.03 ± 0.02	0.1 ± 0.02	0.1 ± 0.1	0.05 ± 0.02	0.1 ± 0.01
18:0/20:4	0.01 ± 0.002	0.01 ± 0.001	0.01 ± 0.003	0.01 ± 0.001	0.1 ± 0.05	0.02 ± 0.003	0.3 ± 0.1	0.1 ± 0.1	0.1 ± 0.01	0.2 ± 0.02	0.1 ± 0.04	0.05 ± 0.01

Figure S11. PG profile of differently treated cells and their EV fractions. Means ± S.E.M. indicate the proportion of individual PG species as percentage of total PG (100%). Heatmaps show fold changes in the proportion of PG species relative to the DMEM control. Data derive from 3 (DMEM, HEPES, ROL+PA, TGF, Ela, DOPC+Ela, S80+Ela, OA, DOPC+OA, S80+OA) or 5 (DOPC, S80) independent experiments. Total lipid concentration for liposomal treatments was 5 mM, Ela or OA concentration 150 nM.

0 1 50 fold change

FFA, cells	DMEM	HEPES	ROL+PA	TGF	DOPC	S80	Ela	DOPC+Ela	S80+Ela	OA	DOPC+OA	S80+OA
	mean ± SEM	mean ± SEM	mean ± SEM	mean ± SEM	mean ± SEM	mean ± SEM	mean ± SEM	mean ± SEM	mean ± SEM	mean ± SEM	mean ± SEM	mean ± SEM
12:0	6.0 ± 1.7	3.3 ± 1.0	3.8 ± 0.5	4.0 ± 0.9	6.1 ± 1.1	3.8 ± 0.8	6.9 ± 1.8	4.2 ± 0.4	4.2 ± 0.5	4.3 ± 0.7	5.3 ± 0.3	4.4 ± 1.0
14:0	4.1 ± 1.1	2.8 ± 0.8	3.1 ± 0.8	3.4 ± 0.8	3.4 ± 0.7	3.5 ± 0.2	3.1 ± 0.8	2.4 ± 0.1	2.4 ± 0.4	2.8 ± 0.5	2.6 ± 0.2	3.9 ± 0.9
16:0	33.0 ± 2.2	36.6 ± 1.5	36.7 ± 1.1	36.2 ± 1.0	33.8 ± 1.3	32.9 ± 2.1	32.2 ± 3.3	36.5 ± 0.2	36.2 ± 1.7	36.8 ± 0.7	35.4 ± 0.8	32.7 ± 2.3
17:0	1.2 ± 0.2	1.0 ± 0.2	0.9 ± 0.1	1.1 ± 0.1	1.1 ± 0.1	1.1 ± 0.1	1.1 ± 0.2	1.0 ± 0.02	0.9 ± 0.1	1.1 ± 0.1	1.0 ± 0.1	2.1 ± 1.1
18:0	47.2 ± 1.2	45.8 ± 1.9	39.1 ± 0.7	44.3 ± 2.5	47.9 ± 1.6	43.0 ± 3.3	44.9 ± 3.7	48.1 ± 1.3	47.4 ± 1.4	44.7 ± 2.5	48.1 ± 1.4	38.1 ± 5.9
14:1	0.9 ± 0.3	0.5 ± 0.3	0.6 ± 0.2	0.7 ± 0.2	0.6 ± 0.1	0.4 ± 0.1	0.4 ± 0.1	0.2 ± 0.04	0.2 ± 0.1	0.3 ± 0.1	0.3 ± 0.04	0.4 ± 0.1
16:1	2.5 ± 0.6	2.5 ± 1.1	7.3 ± 0.5	3.1 ± 0.9	2.0 ± 0.3	2.4 ± 0.6	2.5 ± 0.8	1.3 ± 0.2	1.6 ± 0.5	2.0 ± 0.4	1.4 ± 0.04	6.2 ± 4.1
18:1	4.5 ± 0.6	6.6 ± 0.1	7.3 ± 0.8	6.4 ± 0.5	4.4 ± 0.5	6.6 ± 1.3	7.6 ± 2.9	5.1 ± 0.8	5.3 ± 0.3	6.4 ± 1.0	4.7 ± 0.8	9.9 ± 3.0
18:2	0.5 ± 0.1	0.6 ± 0.02	1.0 ± 0.2	0.7 ± 0.1	0.6 ± 0.2	2.3 ± 0.9	1.2 ± 0.4	0.9 ± 0.2	1.1 ± 0.1	1.4 ± 0.4	1.0 ± 0.1	1.8 ± 0.3
20:3	0.03 ± 0.02	0.03 ± 0.01	0.1 ± 0.05	0.04 ± 0.003	0.01 ± 0.01	0.9 ± 0.6	0.1 ± 0.01	0.04 ± 0.03	0.1 ± 0.02	0.02 ± 0.004	0.1 ± 0.03	0.1 ± 0.04
20:4	0.01 ± 0.01	0.01 ± 0.01	0.02 ± 0.005	0.01 ± 0.004	0.005 ± 0.002	1.5 ± 0.9	0.02 ± 0.01	0.01 ± 0.002	0.3 ± 0.1	0.002 ± 0.002	0.01 ± 0.01	0.2 ± 0.1
20:5	0.004 ± 0.004	0.0 ± 0.0	0.002 ± 0.002	0.01 ± 0.01	0.0 ± 0.0	0.01 ± 0.01	0.002 ± 0.001	0.04 ± 0.02	0.003 ± 0.003	0.0004 ± 0.0003	0.01 ± 0.01	0.0 ± 0.0
22:4	0.01 ± 0.01	0.01 ± 0.003	0.01 ± 0.004	0.004 ± 0.004	0.01 ± 0.01	0.7 ± 0.5	0.0 ± 0.0	0.01 ± 0.003	0.1 ± 0.01	0.001 ± 0.001	0.01 ± 0.01	0.1 ± 0.02
22:5	0.1 ± 0.02	0.1 ± 0.02	0.1 ± 0.02	0.04 ± 0.03	0.05 ± 0.01	0.5 ± 0.3	0.1 ± 0.02	0.1 ± 0.01	0.1 ± 0.01	0.04 ± 0.02	0.1 ± 0.02	0.1 ± 0.02
22:6	0.02 ± 0.01	0.01 ± 0.01	0.01 ± 0.01	0.01 ± 0.003	0.03 ± 0.004	0.2 ± 0.1	0.01 ± 0.01	0.03 ± 0.01	0.05 ± 0.02	0.04 ± 0.002	0.02 ± 0.02	0.04 ± 0.005

FFA, EVs	DMEM	HEPES	ROL+PA	TGF	DOPC	S80	Ela	DOPC+Ela	S80+Ela	OA	DOPC+OA	S80+OA
	mean ± SEM	mean ± SEM	mean ± SEM	mean ± SEM	mean ± SEM	mean ± SEM	mean ± SEM	mean ± SEM	mean ± SEM	mean ± SEM	mean ± SEM	mean ± SEM
12:0	4.9 ± 0.4	3.5 ± 1.1	3.8 ± 1.0	5.0 ± 0.8	3.3 ± 0.8	4.9 ± 0.4	5.6 ± 1.6	5.6 ± 0.4	4.3 ± 1.1	5.7 ± 1.1	5.7 ± 1.0	5.6 ± 0.8
14:0	3.5 ± 0.7	2.7 ± 0.8	3.3 ± 1.1	3.5 ± 0.9	3.0 ± 0.7	3.9 ± 0.6	2.9 ± 0.7	3.1 ± 0.05	3.5 ± 0.6	3.1 ± 0.1	3.8 ± 0.5	3.0 ± 0.4
16:0	35.3 ± 1.6	37.9 ± 1.0	36.6 ± 1.3	35.8 ± 1.3	36.2 ± 0.8	35.0 ± 0.6	32.2 ± 3.2	35.4 ± 0.2	34.2 ± 1.8	33.8 ± 1.0	32.4 ± 1.3	35.6 ± 1.8
17:0	1.3 ± 0.2	0.9 ± 0.01	1.2 ± 0.2	1.1 ± 0.1	1.2 ± 0.2	1.2 ± 0.03	1.3 ± 0.1	1.2 ± 0.1	1.6 ± 0.4	1.2 ± 0.1	1.7 ± 0.3	1.0 ± 0.1
18:0	47.6 ± 1.8	47.8 ± 0.6	47.0 ± 2.7	45.6 ± 2.7	46.5 ± 1.4	45.4 ± 1.5	45.4 ± 6.0	46.4 ± 0.3	43.6 ± 2.2	46.4 ± 1.4	44.9 ± 3.1	46.6 ± 0.5
14:1	0.5 ± 0.1	0.4 ± 0.3	0.5 ± 0.3	0.8 ± 0.4	0.5 ± 0.3	0.7 ± 0.3	0.3 ± 0.1	0.3 ± 0.02	0.4 ± 0.1	0.3 ± 0.1	0.4 ± 0.1	0.3 ± 0.04
16:1	1.7 ± 0.4	1.3 ± 0.4	2.0 ± 1.2	2.8 ± 1.3	2.5 ± 1.0	2.9 ± 0.9	2.5 ± 1.4	1.5 ± 0.2	3.6 ± 1.9	2.3 ± 0.7	3.2 ± 1.4	1.3 ± 0.3
18:1	4.7 ± 0.7	4.9 ± 1.0	4.9 ± 1.0	4.7 ± 0.4	6.1 ± 1.2	4.9 ± 0.6	8.0 ± 4.4	4.7 ± 0.5	6.8 ± 1.2	6.0 ± 1.0	6.4 ± 1.3	5.2 ± 0.4
18:2	0.4 ± 0.1	0.4 ± 0.1	0.5 ± 0.1	0.4 ± 0.1	0.6 ± 0.1	0.9 ± 0.1	1.8 ± 1.1	1.7 ± 0.3	1.8 ± 0.03	1.0 ± 0.05	1.3 ± 0.4	1.1 ± 0.2
20:3	0.01 ± 0.01	0.0 ± 0.0	0.01 ± 0.01	0.003 ± 0.003	0.02 ± 0.01	0.04 ± 0.01	0.02 ± 0.01	0.005 ± 0.005	0.1 ± 0.1	0.01 ± 0.003	0.05 ± 0.02	0.1 ± 0.03
20:4	0.03 ± 0.02	0.0002 ± 0.0002	0.01 ± 0.004	0.02 ± 0.02	0.004 ± 0.003	0.1 ± 0.02	0.01 ± 0.01	0.002 ± 0.002	0.1 ± 0.1	0.004 ± 0.004	0.0 ± 0.0	0.1 ± 0.1
20:5												
22:4	0.01 ± 0.01	0.01 ± 0.01	0.001 ± 0.001	0.01 ± 0.001	0.01 ± 0.004	0.04 ± 0.01	0.001 ± 0.001	0.01 ± 0.01	0.05 ± 0.03	0.005 ± 0.005	0.01 ± 0.01	0.04 ± 0.03
22:5	0.05 ± 0.02	0.1 ± 0.03	0.1 ± 0.01	0.1 ± 0.04	0.1 ± 0.005	0.1 ± 0.01	0.001 ± 0.001	0.1 ± 0.02	0.1 ± 0.03	0.04 ± 0.03	0.1 ± 0.02	0.1 ± 0.1
22:6	0.02 ± 0.004	0.002 ± 0.002	0.03 ± 0.02	0.002 ± 0.001	0.01 ± 0.01	0.02 ± 0.01	0.01 ± 0.01	0.03 ± 0.02	0.03 ± 0.02	0.02 ± 0.01	0.004 ± 0.003	0.02 ± 0.02

Figure S12. FFA composition of differently treated cells and their EV fractions. Means ± S.E.M. indicate the proportion of individual FFAs as percentage of total FFA (100%). Heatmaps show fold changes in the proportion of FFAs relative to the DMEM control. Data derive from 3 (DMEM, HEPES, ROL+PA, TGF, Ela, DOPC+Ela, S80+Ela, OA, DOPC+OA, S80+OA) or 5 (DOPC, S80) independent experiments. Total lipid concentration for liposomal treatments was 5 mM, Ela or OA concentration 150 nM.

Table S1. Detailed One-way ANOVA analysis of variance used to compare means of independent experiments reported in Figure 3b. Significant differences in lipid droplets quantification as function of various treatments were compared by Tukey's multiple comparisons test (**** $p \leq 0.0001$, *** $p \leq 0.001$, ** $p \leq 0.01$, *$p \leq 0.05$).

Tukey's multiple comparisons test	Mean Diff.	95.00% CI of diff.	Below threshold?	Summary	Adjusted P Value	
DMEM vs. HEPES (10%)	0.8779	-19.49 to 21.24	No	ns	>0.9999	A-B
DMEM vs. ROL+PA (10+300 µM)	-21.64	-42.01 to -1.277	Yes	*	0.0304	A-C
DMEM vs. TGF (10 ng/mL)	1.247	-19.12 to 21.61	No	ns	>0.9999	A-D
DMEM vs. DOPC (5 mM)	1.031	-19.33 to 21.40	No	ns	>0.9999	A-E
DMEM vs. S80 (5 mM)	-22.98	-43.34 to -2.610	Yes	*	0.0178	A-F
DMEM vs. ELA (150 nM)	1.178	-19.19 to 21.54	No	ns	>0.9999	A-G
DMEM vs. DOPC+ELA (5 mM + 150 nM)	1.214	-19.15 to 21.58	No	ns	>0.9999	A-H
DMEM vs. S80+ELA (5 mM + 150 nM)	-26.31	-46.68 to -5.944	Yes	**	0.0045	A-I
DMEM vs. OA (150 nM)	0.2644	-20.10 to 20.63	No	ns	>0.9999	A-J
DMEM vs. DOPC+OA (5 mM + 150 nM)	0.4341	-19.93 to 20.80	No	ns	>0.9999	A-K
DMEM vs. S80+OA (5 mM + 150 nM)	-26.9	-47.26 to -6.532	Yes	**	0.0035	A-L
HEPES (10%) vs. ROL+PA (10+300 ¬µM)	-22.52	-42.89 to -2.155	Yes	*	0.0214	B-C
HEPES (10%) vs. TGF (10 ng/mL)	0.3695	-20.00 to 20.74	No	ns	>0.9999	B-D
HEPES (10%) vs. DOPC (5 mM)	0.1532	-20.21 to 20.52	No	ns	>0.9999	B-E
HEPES (10%) vs. S80 (5 mM)	-23.85	-44.22 to -3.488	Yes	*	0.0125	B-F
HEPES (10%) vs. ELA (150 nM)	0.2998	-20.07 to 20.67	No	ns	>0.9999	B-G
HEPES (10%) vs. DOPC+ELA (5 mM + 150 nM)	0.3362	-20.03 to 20.70	No	ns	>0.9999	B-H
HEPES (10%) vs. S80+ELA (5 mM + 150 nM)	-27.19	-47.55 to -6.821	Yes	**	0.0031	B-I
HEPES (10%) vs. OA (150 nM)	-0.6135	-20.98 to 19.75	No	ns	>0.9999	B-J
HEPES (10%) vs. DOPC+OA (5 mM + 150 nM)	-0.4438	-20.81 to 19.92	No	ns	>0.9999	B-K
HEPES (10%) vs. S80+OA (5 mM + 150 nM)	-27.78	-48.14 to -7.410	Yes	**	0.0024	B-L
ROL+PA (10+300 ¬µM) vs. TGF (10 ng/mL)	22.89	2.524 to 43.26	Yes	*	0.0185	C-D
ROL+PA (10+300 ¬µM) vs. DOPC (5 mM)	22.67	2.308 to 43.04	Yes	*	0.0202	C-E
ROL+PA (10+300 ¬µM) vs. S80 (5 mM)	-1.333	-21.70 to 19.03	No	ns	>0.9999	C-F
ROL+PA (10+300 ¬µM) vs. ELA (150 nM)	22.82	2.455 to 43.19	Yes	*	0.019	C-G
ROL+PA (10+300 ¬µM) vs. DOPC+ELA (5 mM + 150 nM)	22.86	2.491 to 43.22	Yes	*	0.0187	C-H
ROL+PA (10+300 ¬µM) vs. S80+ELA (5 mM + 150 nM)	-4.667	-25.03 to 15.70	No	ns	0.9993	C-I
ROL+PA (10+300 ¬µM) vs. OA (150 nM)	21.91	1.541 to 42.27	Yes	*	0.0274	C-J
ROL+PA (10+300 ¬µM) vs. DOPC+OA (5 mM + 150 nM)	22.08	1.711 to 42.44	Yes	*	0.0256	C-K
ROL+PA (10+300 ¬µM) vs. S80+OA (5 mM + 150 nM)	-5.255	-25.62 to 15.11	No	ns	0.9979	C-L

TGF (10 ng/mL) vs. DOPC (5 mM)	-0.2163	-20.58 to 20.15	No	ns	>0.9999	D-E
TGF (10 ng/mL) vs. S80 (5 mM)	-24.22	-44.59 to -3.858	Yes	*	0.0107	D-F
TGF (10 ng/mL) vs. ELA (150 nM)	-0.0697	-20.44 to 20.30	No	ns	>0.9999	D-G
TGF (10 ng/mL) vs. DOPC+ELA (5 mM + 150 nM)	-0.03333	-20.40 to 20.33	No	ns	>0.9999	D-H
TGF (10 ng/mL) vs. S80+ELA (5 mM + 150 nM)	-27.56	-47.92 to -7.191	Yes	**	0.0026	D-I
TGF (10 ng/mL) vs. OA (150 nM)	-0.983	-21.35 to 19.38	No	ns	>0.9999	D-J
TGF (10 ng/mL) vs. DOPC+OA (5 mM + 150 nM)	-0.8133	-21.18 to 19.55	No	ns	>0.9999	D-K
TGF (10 ng/mL) vs. S80+OA (5 mM + 150 nM)	-28.15	-48.51 to -7.780	Yes	**	0.002	D-L
DOPC (5 mM) vs. S80 (5 mM)	-24.01	-44.37 to -3.641	Yes	*	0.0117	E-F
DOPC (5 mM) vs. ELA (150 nM)	0.1466	-20.22 to 20.51	No	ns	>0.9999	E-G
DOPC (5 mM) vs. DOPC+ELA (5 mM + 150 nM)	0.183	-20.18 to 20.55	No	ns	>0.9999	E-H
DOPC (5 mM) vs. S80+ELA (5 mM + 150 nM)	-27.34	-47.71 to -6.975	Yes	**	0.0029	E-I
DOPC (5 mM) vs. OA (150 nM)	-0.7667	-21.13 to 19.60	No	ns	>0.9999	E-J
DOPC (5 mM) vs. DOPC+OA (5 mM + 150 nM)	-0.597	-20.96 to 19.77	No	ns	>0.9999	E-K
DOPC (5 mM) vs. S80+OA (5 mM + 150 nM)	-27.93	-48.30 to -7.563	Yes	**	0.0022	E-L
S80 (5 mM) vs. ELA (150 nM)	24.15	3.788 to 44.52	Yes	*	0.011	F-G
S80 (5 mM) vs. DOPC+ELA (5 mM + 150 nM)	24.19	3.824 to 44.56	Yes	*	0.0108	F-H
S80 (5 mM) vs. S80+ELA (5 mM + 150 nM)	-3.333	-23.70 to 17.03	No	ns	>0.9999	F-I
S80 (5 mM) vs. OA (150 nM)	23.24	2.875 to 43.61	Yes	*	0.016	F-J
S80 (5 mM) vs. DOPC+OA (5 mM + 150 nM)	23.41	3.044 to 43.78	Yes	*	0.0149	F-K
S80 (5 mM) vs. S80+OA (5 mM + 150 nM)	-3.922	-24.29 to 16.44	No	ns	0.9999	F-L
ELA (150 nM) vs. DOPC+ELA (5 mM + 150 nM)	0.03637	-20.33 to 20.40	No	ns	>0.9999	G-H
ELA (150 nM) vs. S80+ELA (5 mM + 150 nM)	-27.49	-47.85 to -7.121	Yes	**	0.0027	G-I
ELA (150 nM) vs. OA (150 nM)	-0.9133	-21.28 to 19.45	No	ns	>0.9999	G-J
ELA (150 nM) vs. DOPC+OA (5 mM + 150 nM)	-0.7436	-21.11 to 19.62	No	ns	>0.9999	G-K
ELA (150 nM) vs. S80+OA (5 mM + 150 nM)	-28.08	-48.44 to -7.710	Yes	**	0.0021	G-L
DOPC+ELA (5 mM + 150 nM) vs. S80+ELA (5 mM + 150 nM)	-27.52	-47.89 to -7.158	Yes	**	0.0027	H-I
DOPC+ELA (5 mM + 150 nM) vs. OA (150 nM)	-0.9497	-21.32 to 19.42	No	ns	>0.9999	H-J
DOPC+ELA (5 mM + 150 nM) vs. DOPC+OA (5 mM + 150 nM)	-0.78	-21.15 to 19.59	No	ns	>0.9999	H-K
DOPC+ELA (5 mM + 150 nM) vs. S80+OA (5 mM + 150 nM)	-28.11	-48.48 to -7.746	Yes	**	0.0021	H-L
S80+ELA (5 mM + 150 nM) vs. OA (150 nM)	26.57	6.208 to 46.94	Yes	**	0.004	I-J
S80+ELA (5 mM + 150 nM) vs. DOPC+OA (5 mM + 150 nM)	26.74	6.378 to 47.11	Yes	**	0.0037	I-K
S80+ELA (5 mM + 150 nM) vs. S80+OA (5 mM + 150 nM)	-0.5888	-20.95 to 19.78	No	ns	>0.9999	I-L

OA (150 nM) vs. DOPC+OA (5 mM + 150 nM)	0.1697	-20.20 to 20.54	No	ns	>0.9999	J-K
OA (150 nM) vs. S80+OA (5 mM + 150 nM)	-27.16	-47.53 to -6.797	Yes	**	0.0031	J-L
DOPC+OA (5 mM + 150 nM) vs. S80+OA (5 mM + 150 nM)	-27.33	-47.70 to -6.966	Yes	**	0.0029	K-L

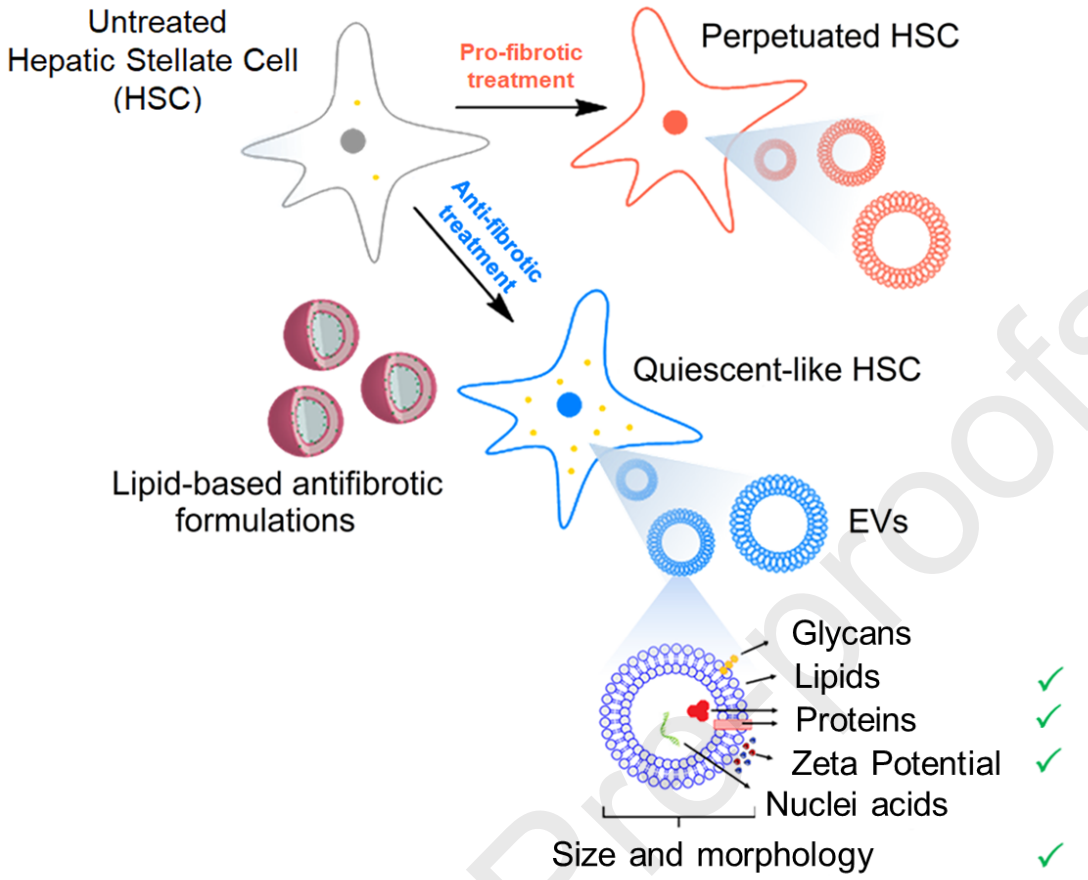

Extracellular Vesicles (EVs) isolation and characterization
➔ evaluation of treatment response